

# **AN ATTEMPT TO SIMULATE TOOL LIFE EQUATION BY RUBBING TESTS**

A Thesis Submitted  
in Partial Fulfilment of the Requirements  
for the Degree of  
**MASTER OF TECHNOLOGY**

By  
**PRADIP KUMAR GHOSH**

*to the*

**DEPARTMENT OF MECHANICAL ENGINEERING**  
**INDIAN INSTITUTE OF TECHNOLOGY KANPUR**  
**MARCH, 1981**

I.I.T. KANPUR  
CENTRAL LIBRARY  
Ref. No. A 66959  
→ 7 SEP 1981

Th  
621.93  
G 346 a

ME-1981-M-GHO-ATT

91.01  
21

## CERTIFICATE

Certified that this work entitled " An Attempt to Simulate Tool Life Equation by Rubbing Tests " has been done by Shri Pradip Kumar Ghosh under my supervision and has not been submitted elsewhere for the award of a degree.

Mohan Krishan Muju ✓

Mohan Krishan Muju  
Assistant Professor  
Department of Mechanical Engineering  
Indian Institute of Technology  
KANPUR-208 016

### POST GRADUATE OFFICE

This thesis has been approved  
for the award of the Degree of  
Mechanical Technology (M.Tech.)  
in accordance with the  
regulations of the Indian  
Institute of Technology KANPUR

Dated. 31.3.81 Q

To  
my parents  
with regards

## ACKNOWLEDGEMENT

The author wishes to place on record, with a deep sense of gratitude, his sincere thanks to -

His thesis supervisor, Dr. M.K. Muju for suggesting the problem, his keen interest, inspiration and able guidance in every stage of doing this work.

Dr. M.M. Oberoi and Dr. G.K. Lal, Department of Mechanical Engineering, for helping the author in carrying out certain analysis.

Members of the technical staff of the department particularly Mr. R.M. Jha, Mr. B.P. Bhartiya and Mr. Joginder Singh for their assistance during the work.

All his friends particularly Messers S. Mukhopadhyay, , S. Dutta, S. Chattopadhyaya, P. Sarkar and others for their direct and indirect help.

Mr. J.P. Gupta for his excellent typing and Mr. B.L. Arora for the beautiful tracings.

Pradip Kumar Ghosh

## CONTENTS

	<u>Page</u>
CERTIFICATE	ii
ACKNOWLEDGEMENT	iii
CONTENTS	iv
LIST OF FIGURES	vi
SYNOPSIS	viii
 Chapter I : INTRODUCTION	1
1.1 Introduction	1
1.2 Cutting Action	2
1.3 Friction in Metal Cutting	3
1.4 Tool Wear	5
1.5 Taylor's Tool Life Equation	9
1.6 Review of Previous Work	14
1.6.1 Types of Rubbing Test	14
1.6.2 Types of Cutting Test	17
1.7 Objective of the Present Work	24
 Chapter II : EFFECT OF CUTTING PARAMETERS ON TOOL LIFE	27
2.1 Effect of Feed on Tool Life	27
2.2 Effect of Depth of Cut on Tool Life	29
2.3 Temperature and Tool Life	29
2.4 Effect of Nose Radius on Tool Life	30
 Chapter III : EXPERIMENTAL RESULTS AND DISCUSSIONS	33
3.1 Experimental Procedure and Setup	33
3.2 Calculation of Pin Wear	37

	<u>Page</u>
3.3.1 Pin Life	42
3.3.2 Effect of Feed	43
3.3.3 Effect of Pin Radius	44
3.3.4 Taper Rubbing Test	46
3.3.5 Coefficient of Friction	47
3.3.6 Calculation of Activation Energy for Resulting Wear	48
Chapter IV: CONCLUSIONS AND SUGGESTIONS FOR FUTURE WORK	64
REFERENCES	66
APPENDIX	69

## LIST OF FIGURES

<u>Fig.No.</u>		<u>Page</u>
1.1	Variation of wear rate with velocity.	7
1.2	Variation of tool wear with cutting time.	7
1.3	View of the crater and flank wear	11
1.4	Pin-Disc mechanism.	15
1.5	Crossed-Cylinder mechanism.	15
1.6	Taylor's Tool Life Relation.	19
1.7	Colding's Tool Life Relation.	19
1.8	Zorev et al. Tool Life Relation.	19
2.1	Effect of cutting variables on tool life.	28
2.2	Effect of nose radius on side cutting edge angle.	31
3.1	Schematic view of the experimental set-up	51
3.2	Variation of wear scar length with rubbing time at different rubbing velocities.	52
3.3	Variation of wear scar length with rubbing time at different rubbing velocities.	53
3.4	Variation of wear scar length with rubbing time at different rubbing velocities.	54
3.5	Variation of wear scar area with time with different rubbing velocities.	55
3.6	Variation of volume of wear with rubbing time at different rubbing velocities.	56
3.7	Rubbing speed-pin life relation (Pin Dia. = 6.35 mm, Feed = 0.05 mm/rev.)	57
3.8	Rubbing speed-Pin life relation (Pin dia. = 6.35 mm, Feed = 0.1 mm/rev.)	58

<u>Fig.No.</u>		<u>Page</u>
3.9	Rubbing speed - Pin life relation. (Pin dia. = 4.4 mm, Feed = 0.05 mm/rev.)	59
3.10	Rubbing speea - Pin life relation. (Volume criterion)	60
3.11	Variation of tool life with nose radius.	61
3.12	Variation of coefficient of friction with rubbing velocity.	62
3.13	Variation of wear rate per unit distance with $1/\theta$ .	63
A-1	Dynamometer details.	
A-2	Calibration chart of dynamometer at a sensitivity of 0.02.	

### SYNOPSIS

The work presented some rubbing tests between H.S.S. pins rubbing against mild steel cylinder at various speeds with the objective of simulating the cutting test flank wear by standard crossed-cylinder wear tests. An attempt has been made to draw an analogy between tool wear and hence tool life equation with pin wear and pin life equation. Effect of various parameters affecting tool life is investigated in pin life tests. The experiments have yielded qualitative agreement between cutting tool wear and crossed cylinder wear system.

With some further suggested work, the procedure can be used as a promising method for rapid tool wear tests.

## CHAPTER I

### INTRODUCTION

#### 1.1 Introduction

Metal cutting is one of the most important ways of processing materials in today's engineering industries. The importance lies in the fact that metal cutting process contribute to share 35 % of the materials consumed each year. The process essentially involves the removal of a layer of metal from the parent blank, thus giving it specified dimensions and surface finish.

The cutting action is very complex in nature which involves plastic deformation resulting from compression, tension and shear. It is achieved by means of a tool, termed as cutting tool, having different angles at the tip. The flow of the material out of the parent blank comes out in the form of chip.

The cost of machined part depends upon many parameters like cost of blank, cost of machining, overhead costs etc. The total cost is the summation of all these individual costs related with the process. One of the important aspects of today's metal machining research is how to decrease the machining cost by increasing productivity. The productivity by itself is directly related to the life of the cutting tool. So the analysis of tool wear and tool life were always of major interest to metal cutting engineers and researchers.

## 1.2 Cutting Action

The cutting action as a whole involves several interacting phenomena. The most important phenomena occurring during the cutting action are plastic deformation, external friction, thermal phenomena in the cutting zone and wear of the cutting tool. It is well accepted now that the predominant mechanism of metal cutting is the metal shearing process occurring in a zone which is called as shear zone.

The process of metal cutting is analysed by the mechanism of chip formation which arises out of the shear deformation of the material being cut. Shearing of the metal, which is responsible for the chip formation, does not occur in a single plane but rather in a finite zone. The actual shear zone is the aggregate of many small shear zones. Although there is a combination of such small shear zones, still the total thickness of these zones is rather small enough. The thickness of the shear zone depends upon the velocity of cutting, the increase in cutting velocity causes the shear zone to decrease [1]. The nature of the shear zone is wedge-shaped comprising of many slip planes where slipping of the deformed material occurs. The plastic deformation does not occur within this shear zone only but it occurs in chip also. As the chip progresses over the tool face, a very thin layer of chip which is in contact with the tool face undergoes additional plastic deformation. This phenomenon is known as secondary shearing.

It arises because of the frictional resistance caused during the sliding of the chip over the tool face. The machined surface under the tool flank also undergoes certain deformation. This happens because of the elastic after effect of the machined surface and the high friction between it and the tool flank. This rubbing of flank with the workpiece is also a cause of tool wear.

### 1.3 Friction in Metal Cutting

As the cutting action progresses, the cutting tool also gets worn out. The basic causes governing the tool wear is the result of frictional rubbing of the chip on the tool face and the rubbing of the workpiece on the tool flank. It also depends upon the amount of pressure to which the cutting point is subjected. Tool wear involves abrasion and removal of microparticles of the surface, as well as microscopic chipping of the cutting edge. Friction and wear of the cutting tool is a bit different from that of the usual machine components. The reason is that in metal cutting, the friction occurs between newly formed nascent surfaces, at high temperature, pressure and comparatively on smaller area of contact. The friction coefficient found in metal cutting is usually higher than the values obtained by direct experiments on surfaces having contaminating films. Further, the coefficient of friction in metal cutting has been found to have a peculiar property of changing with cutting tool geometry [2]. If only the rake angle

of a cutting tool is changed, a wide range of coefficient of friction is obtained. Zorev [3] has found that the coefficient of friction increases with velocity upto certain point then it starts decreasing with increase of velocity.

When a metal slides over another, a sliding resistance results which has been explained to be the combination of three major factors as

- i) mechanical interlocking of the surface asperities,
- ii) ploughing of the surface asperities of the two metals,
- iii) welding of the surface asperities of one metal to the other, resulting in metallic junctions.

In a basic sliding friction case of particular material combination, it is not possible to guess which one out of these three will predominate over other. In metal cutting, however it is believed that frictional resistance is primarily due to the shearing of asperities. Mechanical interlocking and ploughing of surface asperities are having negligible effect [4]. This can be viewed as a fact that in metal cutting, friction occurs at a high normal pressure and as a consequence the ratio of real area of contact to apparent area of contact increases to nearly one which is higher than in conventional sliding friction. Moreover the matching of the nascent surfaces in cutting gives rise to the strong metallic junctions which helps to increase the ratio further.

Although there are ample discussions available in the literature regarding the friction process in metal cutting [5-9], still some of these aspects need further investigations. Kronenberg [9] suggested to split the coefficient of friction into two or more coefficients, one referring to the chip-tool interface and another referring to the internal friction in the shear plane.

#### 1.4 Tool Wear

Tool wear is a very complex phenomena and depends upon many factors. Some of these are : physicochemical properties of the tool and work material, surface conditions at cutting edge of the tool, cutting fluid with its physicochemical properties, cutting variables, rigidity of the machine-fixture-tool-workpiece complex and other machining factors.

In general, tool wear occurs both on the face and the flank of the tool, but depending upon the machining conditions, one of these may predominate over other. Flank wear is characterised mainly by the width of wear land and on the other hand face wear is characterised by depth and width of crater.

The three major causes which are considered to be responsible for tool wear are as follows :

- i) Abrasive action of the hard constituents contained in the work material.
- ii) Adhesion between tool-chip and tool-workpiece combination.

iii) Diffusion between work and tool material.

Oxidation and electrochemical reaction have also been suggested to be responsible for causing the tool wear in certain situations. All these are velocity dependent processes and with increase in velocity one may increase while other decrease.

Fig. 1.1 shows such variation of wear rates with velocity.

## 1. Abrasive Wear

It arises because of the ploughing by the harder constituents present in the matrix of the materials. Harder constituents present in the workpiece material ploughs the softer constituents of the cutting tool material. It depends very much upon the material combination. It can be intuitively said that for the same workpiece material, abrasive wear will be less predominant in carbides than in high speed steel tools. Abrasion is relatively more severe on the tool flank because of the rigid backing provided by the workpiece to the tool flank as compared to the tool face where the contact between thin chip and the tool is not so compact in nature.

## 2. Adhesion Wear

Each and every surface is rough at micro-level and possesses hills and valleys. As a result, when two surfaces come in contact, the real contact takes place in very small isolated places which leads to the real area of contact to be much less than the apparent area of contact. The number of contact points and the normal stress depends upon the applied

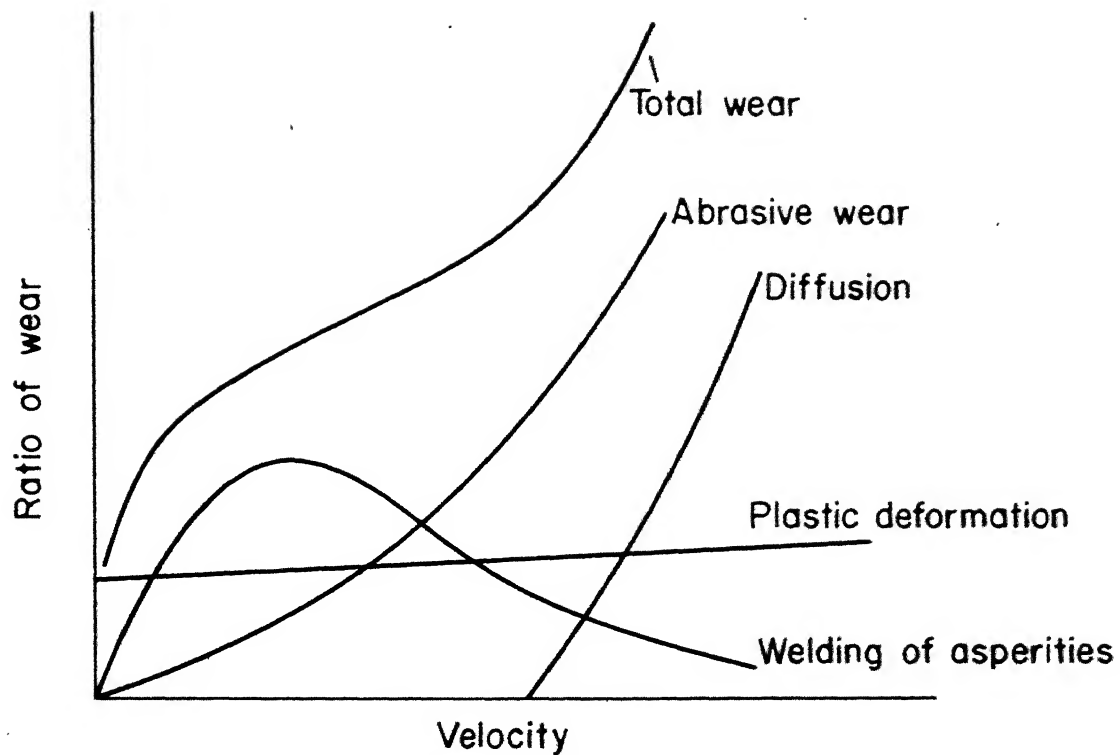


Fig. I.1 Variation of wear rate with velocity

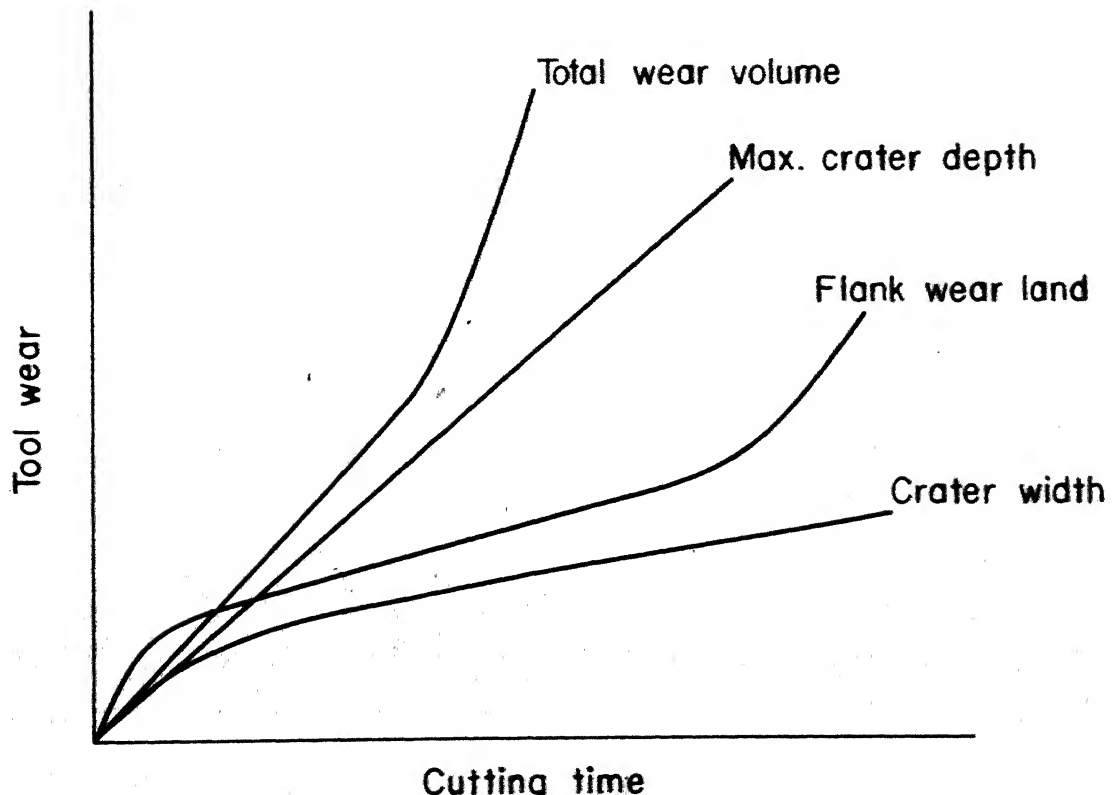


Fig.I.2 Variation of tool wear with cutting time (33)

normal load. When the normal load is very high, the normal stress may exceed the yield point of one or both the materials. The contact area will then weld together to form junctions. These isolated junctions must be broken in order to initiate and sustain relative motion of the two solids. The force necessary to break these junctions is a measure of friction. During the process of junction fracture, wear debris are formed although it is not necessarily true that all the fracture will cause wear debris [10]. This type of welding process can be divided into two classes : pressure weld and temperature weld [11]. A pressure weld may be defined to be a weld which occurs at a temperature below the recrystallization temperature of the softer metal of the pair, while temperature weld occurs when the surface temperature is above the recrystallization temperature.

### 3. Diffusion Wear

Diffusion is a mechanism in which atoms in a metallic crystal shift from one lattice point to another. It occurs as a result of mutual dissolution of the reacting materials of the work-tool pair. Diffusion depends upon time, temperature, strain rate and also on the bonding affinity of material pair. Wear at very high cutting speed is often classified as a case of diffusion wear.

The nature of the variation of the tool wear depends upon the type of wear. The nature of the variation of the flank wear width with time is different to the variation of crater

depth or crater width with time. Fig. 1.2 shows the variation of tool wear with time. Crater depth increases almost linearly with time whereas in the flank wear land, three distinct sections are visible. Section I is the wear-in period (initial wear) during which heavy abrasion of the most salient parts of the surface occurs. Section II is the period termed as normal wear. It is characterized as gradual wear period. Section III can be classified as a period of rapid and destructive wear which arises when the tool gets relatively blunt causing increase in force for cutting.

### 1.5 Taylor's Tool Life Equation

In 1907, Taylor [12] concluded that tool life is related to the cutting speed as

$$VT^n = C$$

where n and C are the emperical constants which depend upon tool work material combination, tool geometry, feed, depth of cut etc. Lot of experimental research work have been carried out since then to find out the effect of other machining variables on the tool life equation.

Tool life can broadly be defined as the useful life of a tool before it ceases to operate effectively. Different criteria have been chosen by different people as the failure of cutting tools. In U.S.A., Europe and Japan, flank wear criterion has been accpeted as the basis of tool life calculations while in

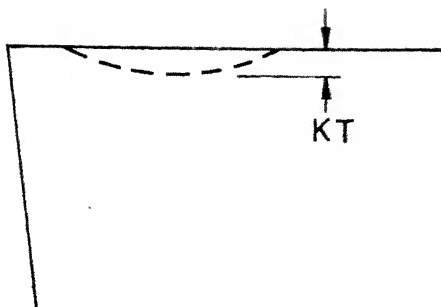
some other countries it is the crater wear criterion. The wear at the flank surface is non-uniform and erratic in nature. The wear at the flank surface can be divided into three regions [Fig. 1.3]. At the tool corner the nature of the wear is more severe because of the complicated flow of chip material at that region. At this region the maximum width of flank wear is designated as  $VC$ . At the opposite end, some times a wear notch is formed which is designated as  $VN$ . This has been explained to be the effect of work-hardening of the workpiece from the previous operation. In the middle portion (Zone B) the wear pattern is usually uniform but some times wear notch can be formed within this region also. The width of the uniform wear within zone B is termed as  $VB$  while the maximum width, if present, is termed as  $VB_{max}$ .

ISO has defined certain criteria for measuring the tool life. Those criteria are as follows :

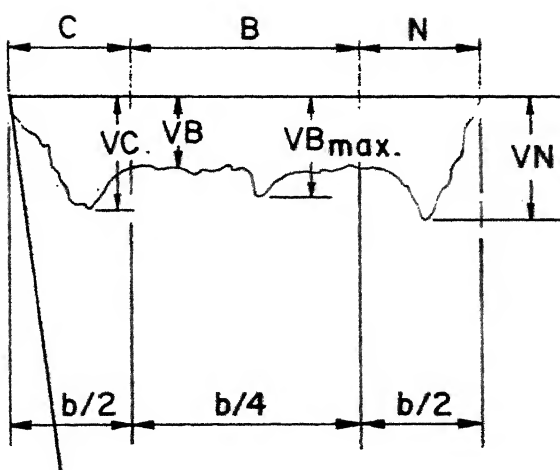
#### Common Criteria for High Speed Steel or Ceramic Tools

The effective tool life for high speed or ceramic tools can be taken as one of the followings.

- i) Catastrophic failure
- ii)  $VB = 0.3 \text{ mm}$  if the flank is regularly worn in zone B
- iii)  $VB_{max} = 0.6 \text{ mm}$  if the flank is irregularly worn, scattered, chipped or badly grooved in zone B



Crater wear



Flank wear

Fig. I.3 View of the crater and flank wear

### Common Criteria for Sintered Carbide Tools

For sintered carbide tool, one of the following criteria can be used.

- i)  $VB = 0.3 \text{ mm}$  if the flank is regularly worn
- ii)  $VB_{\max} = 0.6 \text{ mm}$  if the flank is irregularly worn
- iii)  $KT = 0.06 + 0.3f$ , where  $f$  is the feed.

Besides the above mentioned criteria, different other criteria have also been used as the failure of tool life. A few such criteria are listed below.

1. When the volume of the tool wear reaches certain value.
2. Degradation of surface finish to a specific value.
3. An increase in the feed force to some specific value.

Criterion 1 is commonly being used for radioactive tool life test while criterion 2 is used for finishing cut operation. Uehara [13] calculated the tool life considering the tool wear volume as the criterion of tool failure. He has proposed that tool flank and crater wear can be calculated as,

$$V_f = 0.5 w^2 b \tan \gamma$$

$$V_c = 0.667 C_w \times C_d \times C_t$$

where  $V_f$  and  $V_c$  are volume of flank and crater wear respectively.  $C_w$ ,  $w$  and  $C_d$  are crater wear width, flank wear width and maximum crater depth respectively.  $C_t$  and  $b$  being the breadth of crater and depth of cut respectively. Cook [1] has calculated the

volume of flank and crater wear as,

$$V_f = \frac{w^2 b \tan \delta}{2}$$

and

$$V_c = \frac{2}{3} b d l$$

Where,  $b$  is the width of cut and  $\delta$  is the end clearance angle and  $w$ ,  $d$ ,  $l$  are the width of flank wear, maximum crater depth and average length of crater respectively.

It is now universally accepted that the relation between cutting velocity and tool life is of the form  $VT^n = C$ , where  $n$ ,  $C$  are constants and  $T$  is the time needed for the flank wear to reach a prescribed criteria mentioned earlier. The exponent  $n$  and the constant  $C$  depends upon what the criterion of the tool life is. The exponent  $n$  based on 0.6 mm failure criterion may be different than 0.3 mm failure criterion. Kronenberg [14] has analysed the datas and found that the tool life exponent  $n$  based on crater wear criteria is about half the value found by flank wear criteria. It has been found that tool life using maximum crater depth criterion is more than flank wear criterion which proves that crater wear criterion is less reliable because failure will occur at the flank surface before it appears in the rake face.

## 1.6 Review of Previous Work

Lot of friction and wear experiments of different nature have so far been carried out. The basic aims of these experiments were mainly to find out the influence of various parameters on wear rate, the nature of friction coefficient and the surface conditions. Different types of wear tests have been adopted at different times with the objective of studying the wear process under the influence of various parameters. The standard tests which have been reported in the literature for analysing the wear process are as follows.

### 1.6.1 Types of Rubbing Test

#### 1. Pin-disc mechanism

In this case a circular pin is rubbed against a circular disc in such a manner that the pin axis is perpendicular to the disc surface and parallel to the disc axis. Fig. 1.4 shows the basic features of such mechanism. The variables of the rubbing process are the normal load, velocity of rubbing, material combination etc. The rubbing velocity can easily be changed by changing the rotational speed of the disc. Sometimes instead of a circular pin, a conical pin is also used. Bisson [15] has used the same experimental procedure but instead of a circular or conical pin, he used a spherical rider. In all the cases wear of metal can be determined by weighing the specimen by microbalance or by measuring the dimensions with a microscope.

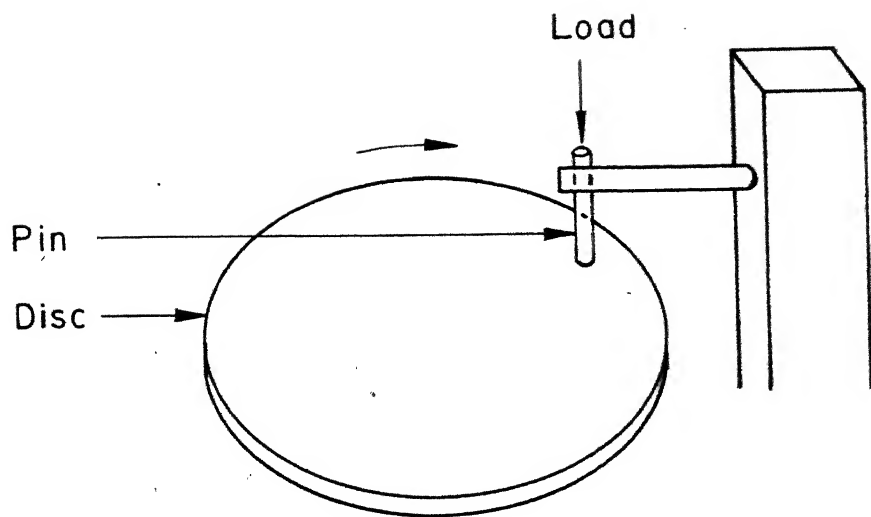


Fig.1.4 Pin - Disc mechanism

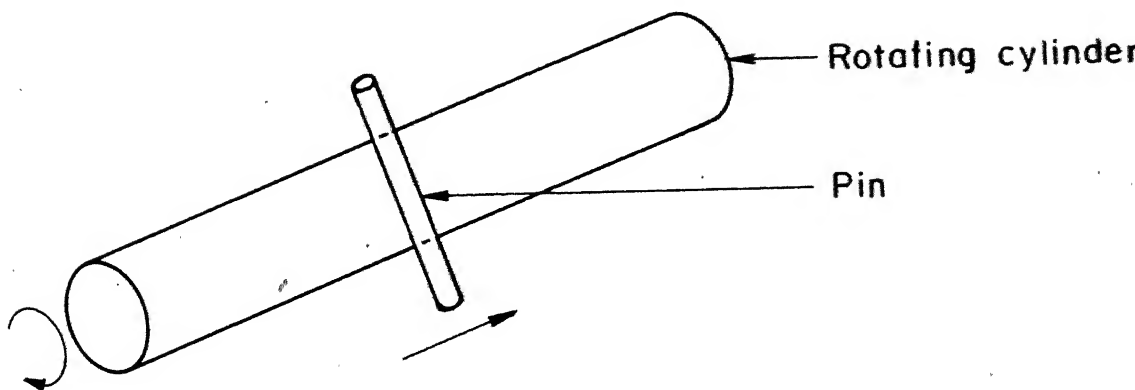


Fig.1.5 Crossed- Cylinder mechanism

Sata [16] has used a bit different mechanism, where he analysed the effect of rubbing on virgin surface and on already rubbed surface. He found that wear in virgin surface increases constantly with time but in repeated rubbing wear becomes more or less constant after sometime. His mechanism was simple but fascinating in nature. He fixed a thick tube on the lathe chuck and made the end face of the cylinder as the rubbing surface. A cutting tool was used to provide a nascent surface prior to rubbing.

## 2. Crossed Cylinder mechanism

This is one of the simplest methods of wear testing and can be done with an ordinary centre lathe. The axes of two cylindrical bodies are made perpendicular to each other, in which one rotates while the other can be given relative linear motion (Fig. 1.5). The fixed cylinder or the pin is pressed onto the rotating cylinder with a predetermined normal load. In this case the profile of the resulting wear scar is elliptical. The dimensions of the wear scar can be measured with an ordinary microscope. Halling [17] has calculated the volume of such wear scar by converging series method and he found the volume V as,

$$V = \frac{\pi}{4} \sqrt{\left[ \frac{a}{b} \right]} \times c^4 \quad (1.1)$$

where, a = radius of rotating cylinder,

b = radius of fixed cylinder,

2c = length of minor axis of wear scar.

### 3. Reciprocating Table mechanism

This mechanism is same as the pin-disc mechanism with the difference that here the relative motion is reciprocating. The pin, whatever may be the shape as cylindrical, conical or hemispherical, is held on to the table with a normal load and the table reciprocates. Precautions are necessary to ensure that the pin does not deflect due to the reciprocating motion of the table.

### 4. Rotating Cylinder mechanism

In this case the pin, either of circular cross section or hemispherical end, is loaded normally on the rotating cylinder surface with a predetermined normal load. Linear relative motion can be given to the fixed pin as in the case of crossed cylinder mechanism.

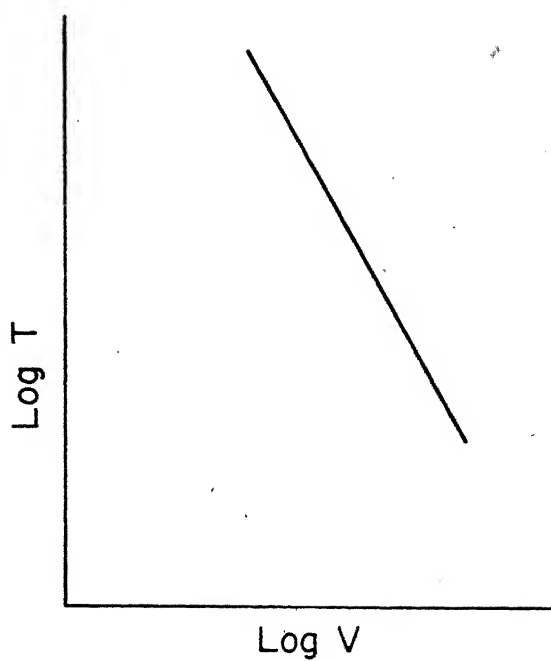
With all the aforesaid wear testing mechanisms various workers have tried so far, the basic aim has been to relate the different parameters like velocity, normal load, interface temperature with the wear rate or to examine the nature of coefficient of friction.

#### 1.6.2 Types of Cutting Test

In cutting test also it has been tried to relate the wear of cutting tool with different parameters. Cutting tool wear is a bit different and complicated in nature than the wear process in the above basic wear tests. This is specially true

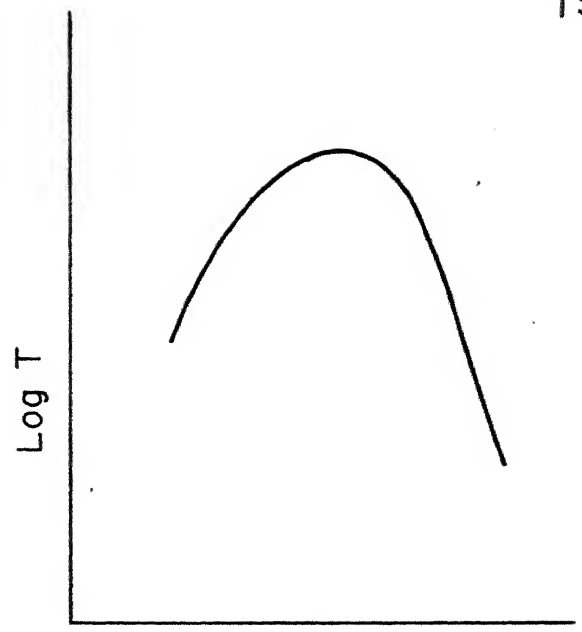
in the case of crater wear. But the basic physics of the flank wear is more or less similar to the conventional rubbing wear. The usual way of analysing the cutting tool wear is from the view point of cutting tool life. Taylor [12] in his famous paper "On the art of cutting metals", has established the relationship between tool life and velocity in 1907. He measured the tool wear at different time and velocities and fixed the flank wear criterion to be the measure of tool life. By plotting the cutting velocities with time on a log-log paper, he found the relationship to be a straight line (Fig. 1.6). Later Colding [18] and Zorev [19] used the same procedure and found that the relationship is not a single straight line over all the region. Colding came up with the conclusion that tool life decreases with speed and follows almost a straight line at higher velocities and it increases with speed at lower velocities (Fig. 1.7). Zorev found that tool life decreases with increase in velocity but in different manner in different zones. He suggested two different zones, one is at higher cutting speed where tool life is more velocity sensitive and another at lower cutting speed where it is relatively less velocity sensitive (Fig. 1.8). Recently Barrow [20] has conducted the same test and found that the relationship follows as found by Colding.

The usual technique of finding the relationship between tool life and velocity is very time consuming and lot of material removal is associated with the process. Having accepted that the relationship obeys Taylor's type equation within a particular



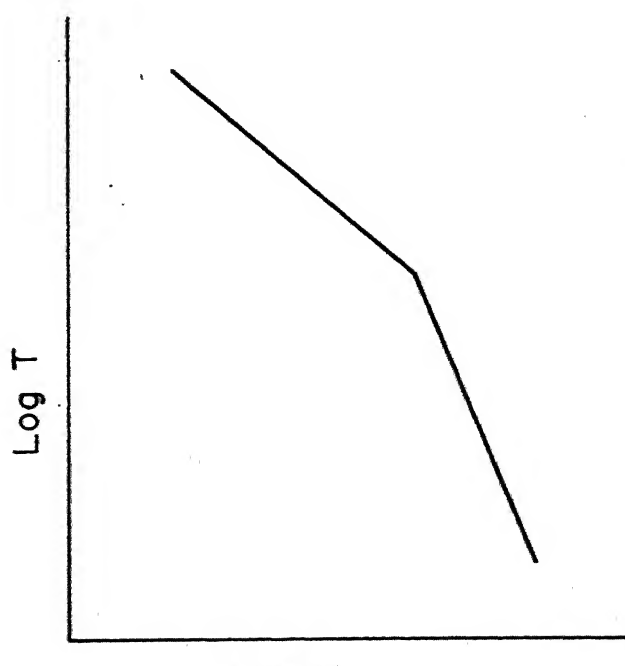
Suggested by Taylor (12)

Fig. I.6



Suggested by Colding (18)

Fig.I.7



Suggested by Zorev et. al.(19)

Fig. I.8

zone, different rapid testing techniques have been derived for finding out the Taylor's tool life equation constants.

### 1. Tool Life Testing by Facing Test

Kraus et. al. [21] have carried out facing test as means to find out the Taylor's tool life equation exponents rapidly. In facing test the cut starts at the centre of the face of a bar and moves radially outward. For a particular r.p.m., the radius at which the tool fails is measured. It can be shown that in a facing test, relationship obeys the form [1],

$$NR^m = K$$

where, N is the spindle speed, R is the radius at which the tool fails and K is a constant. The constants m and K can be equated as,

$$m = \frac{1+n}{1-n}$$

$$K = \left[ t \left( \frac{n+1}{n} \right) \right]^{n/(1+n)} \left[ \frac{12 C}{2\pi} \right]^{1/(1-n)}$$

where, t is the feed rate, n is the Taylor's exponent and C is the Taylor's constant.

Solaja [22] also carried out the facing test and found the values of n and C close to the conventional test values. He did the experiment at two different spindle speeds  $N_1$  and  $N_2$

and measured the radius at which the tool failure occurred. He calculated the Taylor's exponent n from the following equation.

$$n = \frac{1}{\frac{\log N_2 - \log N_1}{2(\frac{\log V_{N_2} - \log V_{N_1}}{\log N_2 - \log N_1})} - 1}$$

where,  $V_{N_1}$  and  $V_{N_2}$  are the speeds at the diameters where the tool failure occurred.

## 2. Taper Turning Test

Heginbotham and Pandey [23] have criticised the above method by pointing out that the composition variation is maximum from the centre to the surface of a bar. They have suggested a different method for finding out the exponent n and constant C rapidly. They derived that X, the fraction of tool life is related to other variables as,

$$X = \left( \frac{\pi N}{6C} \right)^{1/n} \cdot \frac{n}{n+1} \cdot \frac{L}{N f} \cdot \frac{\frac{R_A}{R_A} - \frac{R_B}{R_B}}{(n+1)/n - (n+1)/n} \quad (1.2)$$

where, L = Taper length, ft.

N = Spindle speed, r.p.m.

f = Feed rate

$R_A, R_B$  = Radius of taper at the end and start of the experiment respectively

$n$  = Taylor's exponent

and  $C$  = Taylor's constant.

If two tests are performed at two different spindle speeds  $N_1$  and  $N_2$  over the same taper length  $L$  and at the same feed rate  $f$ , then  $n$  can be calculated as,

$$n = \frac{1}{\left( \log \frac{X_1}{X_2} / \log \frac{N_1}{N_2} \right) + 1} \quad (1.3)$$

where,  $X_1$  and  $X_2$  are the fractions of tool life related to spindle speeds  $N_1$  and  $N_2$ . If  $M$  number of passes required to reach a wear land of  $W_M$  and the failure criterion is  $W_0$ , then  $X$  can be expressed as,

$$X = \frac{W_M}{MW_0}$$

### 3. Variable Rate Machining Test

Taper turning test also suffers to some extent from the drawback of variation of composition of the bar stock. In order to get rid of this disadvantage completely, Heginbotham and Pandey [24] also suggested a different technique for finding out the Taylor's exponents. In this experiment they continuously varied the spindle speed as the cutting progressed. Taking two sets of conditions,  $D_1, L_1, V_{B_1}$  and  $D_2, L_2, V_{B_2}$  at a particular feed rate and maintaining the condition  $K_1 = K_2$

where  $K = V_A/V_B$ , the Taylor's exponent can be found out as,

$$n = \frac{1}{\frac{\log \alpha}{\log \beta} + 1}$$

where,

$$\alpha = \left[ \frac{X_1 \cdot D_2 \cdot L_2}{X_2 \cdot D_1 \cdot L_1} \right]$$

and

$$\beta = \frac{V_{B_1}}{V_{B_2}}$$

The variable rate machining test takes less amount of material than taper turning test and does not suffer the disadvantages of material fluctuations although in both the two cases the results are well satisfactory.

The following table gives the comparison of taper turning test and variable rate machining test with the conventional method of tool life testing.

TABLE 1.1

Testing Technique	Weight of material consumed	Testing time	Number of test tools used
Conventional	135 Kg.	3 hr. 23 min.	6
Taper turning	45 Kg.	1 hr. 45 min.	2
Variable rate machining	20 Kg.	35 min.	2

#### 4. Step Turning Test

Kiang and Barrow [25] have suggested step turning test where they modified variable rate machining test by a large number of small constant speed steps. They shown Taylor's exponent n to be as,

$$n = \log \left( \frac{V}{V_0} \right) / \log \left( \frac{Gt'}{G_0 t} \right)$$

where,

$$G = \frac{\text{amount of mean flank wear reached in time } 't'}{\text{mean flank wear}}$$

Although the rapid tool life test methods are approximate in nature, their values gave quite satisfactory results for finding out the exponents. The major assumption in all these tests are that the velocity vs. tool life curve over a log-log paper is a straight line over that particular range which is ofcourse a resonable assumption because of its verification by so many other researchers.

#### 1.7 Objective of the Present Work

The objective of the present work was to investigate whether an appropriate rubbing test alone instead of a cutting test could be attempted to simulate the actual cutting tool life tests. The basis for the proposed runs as follows.

Wear at the flank of a cutting tool is a consequence of an intence rubbing of the tool flank with the machined surface.

The machined surface is in a state of strain hardened condition and subjected to thermal effects at the same time. The gross plastic deformation at the cutting edge generates considerable amount of heat, part of which flows to the tool flank. Also, an enormous stress is present at the tool point. In order to simulate the effect of the actual cutting action on the flank by a rubbing test alone, it is necessary that conditions at the rubbing interface are also exactly similar. Therefore proper simulating rubbing test would apparently be quite involved.

In the present work an attempt has been made to cover the initial ground in this direction, in order to explore usefulness of the idea. The objective was to explore if Taylor's tool life constants can be predicted from a rubbing test between a pin and a cylinder representing tool-work combination. The plan of the experiment was as follows.

Pins of H.S.S. would be rubbed against a mild steel cylinder at various speeds, feeds and operating load. The growth of the pin wear with time would be recorded as in the case of tool wear tests. An appropriate magnitude of pin wear would be taken as a criterion of "pin life" to investigate if an equation of the type  $VT^n = C$  would be realised and if so, with what values of n and C. Such an investigation would perhaps form the basis for further appropriate experiments to obtain closeness of n and C values between rubbing and cutting for a given material combination.

If such an appropriate rubbing test could be designed, the obvious advantage would be considerable saving of material consumption as well as in the number of tools because rubbing tests consume negligible material.

It may not be very easy to simulate the effect of tool geometry exactly in the pin type rubbing test. Nevertheless keeping in mind that the suitable tool geometry has been standardized now, one does not have to investigate a very wide range. With reasonable effort appropriate pin and cylinder sizes and other parameters should be identifiable which would take care of the tool geometry of the practical range of interest.

The literature survey does not readily show any work attempted to obtain Taylor's tool life equation constants by rubbing tests. It was therefore considered to be quite appropriate to explore the possibility of such tests. Hence, the justification for the present work.

## CHAPTER II

### EFFECT OF CUTTING PARAMETERS ON TOOL LIFE

#### 2.1 Effect of feed on Tool Life

Several workers have suggested relationships relating tool life with cutting speed, feed and depth of cut. The general form of such equation is of the type,

$$T = A \cdot V^{-B} f^{-C} t^{-D} \quad (2.1)$$

where,

$T$  = tool life

$V$  = cutting speed

$f$  = feed rate

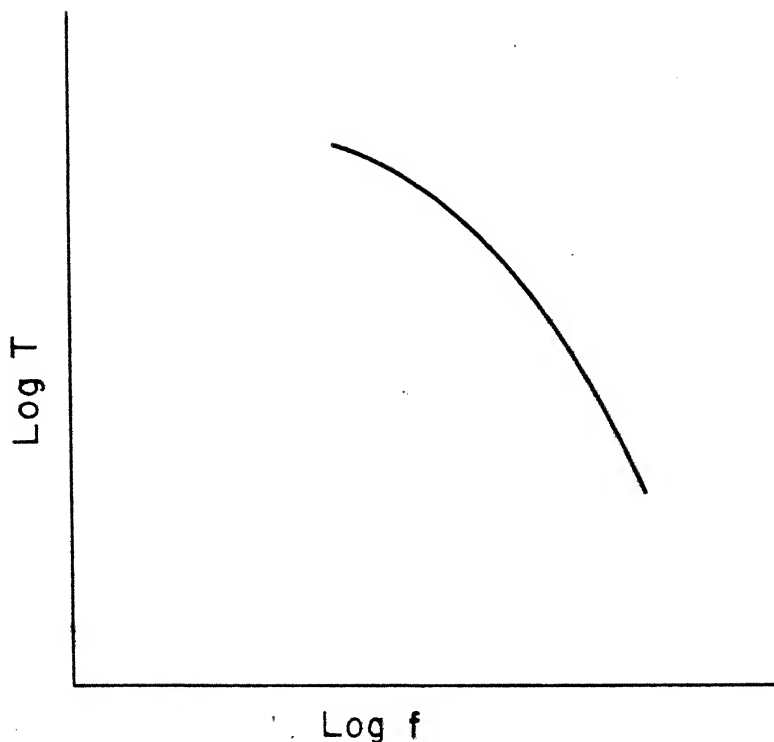
$t$  = depth of cut.

$A$ ,  $B$ ,  $C$ ,  $D$  are emperical constants.

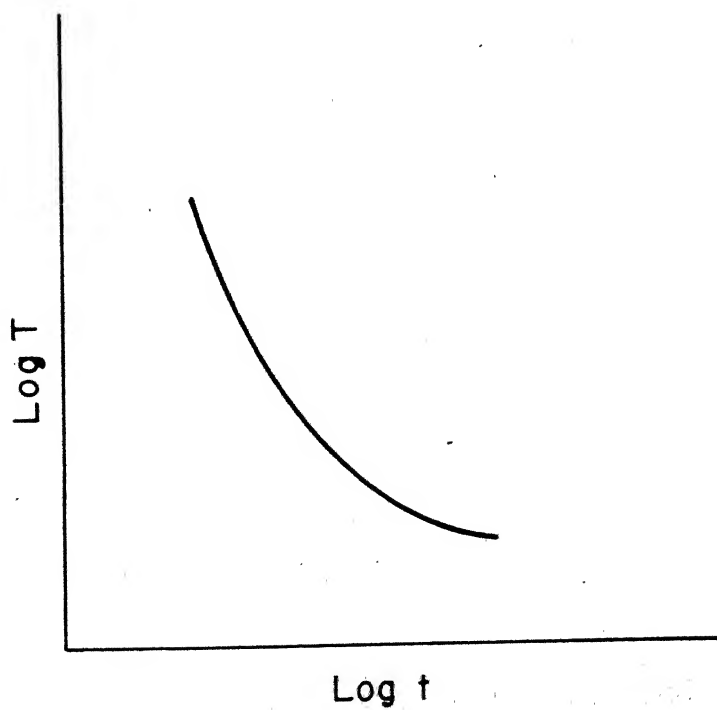
The equation can be rearranged for a constant depth of cut and is generally written as,

$$V T^n f^m = C \quad (2.2)$$

where,  $n$ ,  $m$  and  $C$  are emperical constants. It has been found by researchers that with increase in feed  $f$  the exponent  $n$  remains almost unchanged but  $C$  decreases. Effect of feed is much more severe on  $C$ . Cook [26] has plotted the  $V_{30}$  values with feed and found that the relationship follows a straight line. The general trend of the effect of feed, depth of cut on tool life



Effect of feed on tool life



Effect of depth of cut on tool life

Fig.2.1 Effect of cutting variables on tool life (20)

as shown by Barrow [20] are given in Fig. 2.1.

## 2.2 Effect of Depth of Cut on Tool Life

Regardless of the criterion of tool failure, it is a well accepted fact that tool life varies most with velocity and feed and depth of cut have much less effect. The variation of tool life with depth of cut is not gentle one, but severe in nature. Depth of cut is related with tool life and velocity by,

$$V T^{-\frac{n_1}{m_1}} t^{\frac{m_1}{n_1}} = C_1 \quad (2.3)$$

where  $n_1$ ,  $m_1$  and  $C_1$  are all emperical constants which depend upon different machining variables. For the same velocity and feed rate, tool life decreases sharply with increase in depth of cut beyond a certain value. Fig. 2.1 shows the relationship between tool life and depth of cut.

## 2.3 Temperature and Tool Life

Olberts [27] carried out extensive research relating resultant tool temperature with the velocity of cutting. He found that at higher cutting speed, the relationship of tool temperature with velocity is of the form

$$\Theta = C_0 V^{n_0} \quad (2.4)$$

where,  $\Theta$  is the temperature of tool and  $V$  is the velocity of cutting,  $n_0$  and  $C_0$  being emperical constants. Several other workers have also confirmed this equation. Kronenberg [14] carried out dimensional analysis and found that the relationship

between temperature, velocity and tool life follow a complicated relation like,

$$T = \left[ \frac{T_e e^{\pi H^{0.5}}}{A^m \cdot K_s \cdot C_1 \cdot v^{(1-2m)}} \right]^{1/(0.5-2m)} \quad (2.5)$$

Where,

$T$  = Tool life

$T_e$  = Temperature

$H$  = Volumetric sp.heat of work material  $\times$  th.  
conductivity of work material.

$A$  = Chip cross section area.

$K_s$  = Unit cutting force.

$C_1$  is the emperical constant and  $m$  being the exponent.

## 2.4 Effect of Nose Radius on Tool Life

It has been found by Sen and Bhattacharyya [28] that tool life of H.S.S. tools cutting SAE-2346 steel, is related to nose radius and velocity by the expression

$$V T^{0.0927} = 331 R^{0.244} \quad (2.6)$$

where,  $R$  is the nose radius.  $V$  and  $T$  are the velocity of cutting and tool life respectively. The expression suggests that with increase in nose radius, tool life also increases. Fig.3.11 shows the plotting of  $V_{60}$  values with different nose radius [29]. It also shows that velocity for 60 min. tool life increase with increase in nose radius, on the other hand decrease of nose radius decreases tool life.

Fig.2.2 shows a tool of nose radius  $r$  adjusted to give a depth of cut  $t$  and having the end cutting angle  $\phi_1$  and side cutting

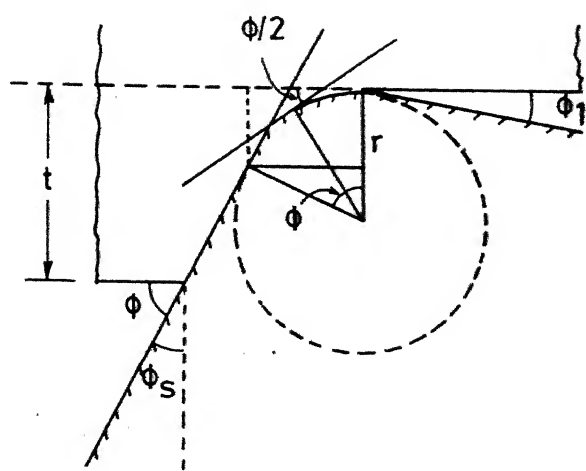


Fig. 2.2 Effect of nose radius on side cutting edge angle.

edge of  $\phi_s$ . The nose radius is provided essentially to strengthen the cutting point but the introduction of nose radius changes the mean value of the principal cutting edge angle. Using Fig. 2.2 it has been shown [28], that the equivalent cutting edge angle  $\phi_{avg}$  can be evaluated as,

$$\phi_{avg} = \frac{\frac{[t + r \cos \phi - r] \phi + r \phi \cdot \frac{\phi}{2}}{\sin \phi}}{\frac{[t + r \cos \phi - r]}{\sin \phi} + r \phi} \quad (2.7)$$

Thus for a given  $\phi$  the equation clearly shows that  $\phi_{avg}$  varies with  $\frac{t}{r}$  ratio. It can be seen using this equation that when everything else remain same, reduction of nose radius would result in increase of  $\phi_{avg}$  or decrease of  $\phi_s$ .

Boston [30] has further derived the relation for HSS tools.

$$V T^{0.11} = 78(\phi_s + 15^\circ)^{0.264} \quad (2.8)$$

where,  $\phi_s$  is the side cutting edge angle.

So decrease of  $\phi_s$  corresponds to decrease of the constant C in Taylor's tool life equation. So it can be concluded that decrease of nose radius will cause Taylor's constant C to decrease. It will be seen in Chapter III that this trend is obtained in pin life test also.

## CHAPTER III

### EXPERIMENTAL RESULTS AND DISCUSSIONS

#### 3.1 Experimental Procedure and Setup

In order to simulate the flank wear of cutting tools by rubbing tests, the following experiments have been performed in the present work.

1. Rubbing of H.S.S. pins of 6.35 mm diameter against mild steel cylinder at feed rates of 0.05 mm/rev. and 0.1 mm/rev.
2. Rubbing of H.S.S. pins of diameter 4.4 mm against the mild steel cylinder at a feed rate of 0.05 mm/rev.
3. Rubbing of H.S.S. pins of 6.35 mm diameter against a tapered mild steel cylinder.

Hot rubbing tests under above conditions were also considered to be done but due to the limited time it could not have been taken up in the present work.

In all these experiments, a constant normal load of 20 Kg. was applied throughout the test. The pin and the cylinder combination represented a crossed-cylinder mechanism (Fig. 1.5). A wide range of velocities (36.13 m/min. to 144.51 m/min.) was chosen for the experiments. Appendix 1 shows the design of the dynamometer which was originally considered to be used in the present work. A different loading system was thought to be used in the experiments. However, when this system was actually

employed, there were considerable vibrations associated with it due to which it was found necessary to use a different system. Fig. 3.1 shows the final setup which was eventually found to be convenient and satisfactory.

In the new system, a spring loaded mechanism was used to keep the radial load constant throughout the experiment. This was made possible by using a spring of relatively low spring constant in which the deflection per kg. load was reasonably large. As the depth of the wear scar was very small, the little deflection of the spring during the experiment caused almost no effect on the radial load. Thus, the system provided a constant load arrangement. The spring loaded arrangement on the other hand gave a very smooth demping effect to the vibration which might be caused due to the surface micro-irregularities or out of roundness of the moving shaft.

The rubbing experiments were always carried out between fresh surfaces and it was ensured that there was no repeated rubbing. Each and every time a fresh surface for rubbing was prepared prior to the experiment. High speed steel pins were rubbed against a mild steel cylinder of 115 mm diameter. The two cylinders axes were made perpendicular to each other so that there was a point contact between the cylindrical surfaces at the beginning of the experiment.

The resulting wear pattern was elliptical in nature and the dimensions of the wear scar were measured by MP320 Carl Zeiss

Optical Projector. It was found during the experiments that wear patterns below 10 min. of rubbing were not of good shape. So, readings below 10 min. have not been recorded because in order to measure the dimensions of the wear scar accurately, it is highly necessary to get well defined contour of the wear scar. Thus wear scar had been measured from 10 min. to 35 min. in six steps. Incidentally, this problem is also associated in measurement of flank wear.

The machine used for doing this experiment was HMT lathe - model LB25. Certain attachments were designed for the application of constant radial load. Fig. 3.1 shows the schematic diagram of such an arrangement. The tool post was taken out of the compound rest and the dynamometer was placed in its place. A specially designed pin holder was used to hold the H.S.S. pin in tangential position to M.S. mild steel workpiece, with the axes of pins and cylinder perpendicular to each other.

The power screw of the compound rest was disengaged and the axis of the compound rest was put parallel to the axis of the cross slide. Compound rest was then made free to slide along the axis of the cross slide. It was then held to the rear tool post by means of the spring. The required load of 20 kg. was applied by means of the spring by adjusting the cross slide appropriately. The details of the machine and instruments used are as follows.

### The Lathe

HMT LB25 lathe was used for the experiment. It is having the following details.

Horsepower	7.5 H.P.
Speeds	32-1600 r.p.m. $r = 1.25$
Feeds	0.05 mm/rev. - 1.4 mm/rev.
Bed length	6 ft.

### The Dynamometer

It was an imported three component Lebow dynamometer, which was used during the experiment. The calibration curves showed exactly linear relationship.

### The Recorder

The recorder used was an Encardio-rite recorder, to measure the forces in X, Y, Z directions simultaneously. Supply voltage of 5 Volts was used during the experiment.

### The Optical Projector

The wear scar was measured with a MP320 Carl Zeiss Optical Projector. The application of this projector lies in measuring the profiles of small workpiece, jigs and fixtures dimensions etc. It has got the following ratings.

Magnification available	10, 20, 50, 100
Distortion by objectives	0.3 %
Distortion by total device	0.5 %
Diameter of projection face	320 mm

### 3.2 Calculation of Pin Wear

The equation of the two cylinders whose axes are perpendicular to each other can be written as:

$$Z^2 + Y^2 = R^2 \quad (3.1)$$

$$X^2 + (Z - (R + r - h))^2 = r^2 \quad (3.2)$$

where,  $R$  = Radius of rotating cylinder

$r$  = Radius of pin

$h$  = maximum depth of wear scar.

#### Volume

The axis of the rotating cylinder being parallel to the X axis and the axis of the pin is parallel to the Y axis. The volume of the wear scar is bounded by the two cylindrical surfaces, the upper surface of the rotating cylinder and the lower surface of the pin. From Eq. (3.1),

$$Z = \pm \sqrt{R^2 - Y^2}$$

From Eq. (3.2),

$$Z = (R + r - h) \pm \sqrt{r^2 - X^2}$$

So, the volume  $V$  of the wear scar is,

$$V = 4 \iint_D [V(R^2 - Y^2) - ((R+r-h) - \sqrt{r^2 - X^2})] dx dy$$

$$\begin{aligned}
 V &= 4 \int_L^C [V(R^2 - Y^2) - (R+r-h) + V(r^2 - X^2)] dx dy \\
 &= 4 \int_0^C dy \int_0^Y [V(R^2 - Y^2) - (R+r-h) + V(r^2 - X^2)] dx
 \end{aligned}$$

Limit

$$V(R^2 - Y^2) = (R+r-h) - V(r^2 - X^2)$$

$$X^2 = r^2 = [(R+r-h) - V(R^2 - Y^2)]^2$$

$$X = \pm (r^2 - [(R+r-h) - V(R^2 - Y^2)]^2)^{1/2}$$

$$= FY$$

$$\begin{aligned}
 V &= 4 \int_0^C dy \left[ X V(R^2 - Y^2) - (R+r-h)X + \frac{r^2}{2} \arcsin \frac{X}{r} \right. \\
 &\quad \left. + \frac{X}{2} V(r^2 - X^2) \right] \Big|_0^{FY} \\
 &= 4 \int_0^C [FY V(R^2 - Y^2) - (R+r-h)FY + \frac{r^2}{2} \arcsin \frac{FY}{2} \\
 &\quad + \frac{FY}{2} V(r^2 - FY^2)] dy
 \end{aligned}$$

$$\begin{aligned}
 &= 4 \int_0^C [(r^2 - (b - V(R^2 - Y^2)))^2]^{1/2} V(R^2 - Y^2) - b(r^2 - (b - V(R^2 - Y^2)))^2 \\
 &\quad + \frac{r^2}{2} \arcsin \frac{(r^2 - (b - V(R^2 - Y^2)))^2}{2}^{1/2} + \frac{(r^2 - (b - V(R^2 - Y^2)))^2}{2}^{1/2} \\
 &\quad \times V(r^2 - (r^2 - (b - V(R^2 - Y^2)))^2)] dy \tag{3.3}
 \end{aligned}$$

where,  $b = R+r-h$

To find C

$$\sqrt{R^2 - Y^2} = b - \sqrt{r^2 - X^2}$$

$$R^2 - Y^2 = (b - \sqrt{r^2 - X^2})^2$$

$$Y = \pm (R^2 - (b - \sqrt{r^2 - X^2}))^{2/2}$$

$$Y \leq \pm (R^2 - (b - r)^2)^{1/2}$$

$$\leq \pm (R^2 - (R - h)^2)^{1/2}$$

$$= C$$

### Surface

In a similar manner, surface area of the wear scar A can be written as,

$$A = 4 \iint_D \sqrt{1 + \left(\frac{\partial Z}{\partial X}\right)^2 + \left(\frac{\partial Z}{\partial Y}\right)^2} dx dy$$

$$Z = + \sqrt{R^2 - Y^2}$$

$$\frac{\partial Z}{\partial X} = 0 \quad \frac{\partial Z}{\partial Y} = - \frac{Y}{\sqrt{R^2 - Y^2}}$$

$$A = 4 \iint_D \sqrt{1 + \frac{Y^2}{R^2 - Y^2}} dx dy$$

$$= 4R \iint_D \frac{dx dy}{\sqrt{R^2 - Y^2}}$$

$$\begin{aligned}
 A &= 4R \int_0^C dy \left\{ \frac{X}{\sqrt{(R^2 - Y^2)}} \right\} \Big|_0^{FY} \\
 &= 4R \int_0^C \frac{FY}{\sqrt{(R^2 - Y^2)}} dy \\
 &= 4R \int_0^C \frac{(r^2 - (b - \gamma(R^2 - Y^2)))^{1/2}}{\sqrt{(R^2 - Y^2)}} dy \quad (3.4)
 \end{aligned}$$

Equations (3.3) and (3.4) are the exact solutions for calculating volume and surface area of the wear scar. As it is difficult to handle the above two equations analytically, numerical method was adopted.

Simpson's one third rule was used for calculating the integrals and it has been found the values agree with the method shown by Hailling [17] and Muju [31]. A computer programming for calculating the above two integrals has been given in Appendix.

### 3.3 Results and Discussions

The length of the major axis, the surface area and the volume of the wear scar have been plotted against rubbing time. Fig. 3.2 shows the length of the major axis of the wear scar vs. rubbing time curve at seven different rubbing velocities and at a feed rate of 0.05 mm/rev. The range of the velocities used was 36.13 m/min. to 144.51 m/min. Fig. 3.3 shows the variation of the length of the major axis of the wear scar with rubbing time for the same diameter of H.S.S. pin (6.35 mm) but

at double the feed rate (0.1 mm/rev.). The effect of feed on the wear mechanism can be analysed with the help of these curves. In both these two cases all the rubbing variables except the feed rate remained constant.

The effect of pin diameter on the wear process can be discussed with the aid of Fig. 3.2 and Fig. 3.4. In Fig. 3.4, length of the wear scar has been plotted against rubbing time for a different pin diameter of 4.4 mm and at a feed rate of 0.05 mm/rev. Fig. 3.2 shows the same variation with a pin diameter of 6.35 mm., other variables remained same.

It is interesting to observe that the nature of these wear growth curves follows the general pattern of the flank wear curve (Fig. 1.2) in machining, within the normal wear zone. The pin wear growth curve can not be compared with the crater wear growth curve because wear takes place in the face of the tool in a different manner i.e. by the action of the hot chip rubbing on the face of the tool where diffusion is predominant. Crater wear differs from the wear of simple rubbing mechanism, where diffusion is of negligible order, at low speeds.

Fig. 3.5 shows the variation of wear scar area with the rubbing time. The wear scar area was calculated using Eq. 3.4. The variation of the volume of the wear scar is plotted in Fig. 3.6, where the pin diameter was 6.35 mm and the feed rate 0.05 mm/rev. Volume of the wear scar zone has been calculate using Eq. 3.3.

### 3.3.1 Pin Life

#### 1. Wear Scar Length Criterion

One of the important aspects of the present work is to evaluate how "pin life" varies with velocity, as understood in cutting process. The aim of doing this is to simulate the wear process of cutting tool wear by the crossed cylinder system of rubbing. The criteria of choosing the tool failure have been discussed in Chapter 2 in a detail. For fixing the "pin life" it has been found convenient to accept 5 mm length of major axis of the wear scar to be the criteria of pin failure. All the wear data have been analysed by fixing the 5 mm wear scar length as a failure criterion.

The times of rubbing corresponding to 5 mm wear scar length have been noted from Fig. 3.2 for various velocities and are plotted on log-log paper. Fig. 3.7 shows such plotting which indicates the variation of "pin life" with rubbing velocities. The variation indeed follows a straight line which suggests an equation similar to Taylor's cutting tool life equation. This necessarily helps to conclude that the basic rubbing wear in crossed cylinder mechanism also follows Taylor's type equation. Calculation for n and C from Fig.3.7 suggests the equation

$$V_T^{.854} = 1106$$

## 2. Wear Scar Volume Criterion

Fig. 3.10 shows the relationship of "pin life" with rubbing speed where the criterion of failure is volume of wear scar. The value of pin failure was fixed to be  $0.125 \text{ mm}^3$  which corresponds to the wear scar volume at 5 mm major axis length. The value of rubbing time corresponding to  $0.125 \text{ mm}^3$  of wear was noted from Fig. 3.6 at different velocities. In this case the diameter of pin and feed rate used were 6.35 mm and 0.05 mm/re. respectively. Variation of "pin life" with rubbing speed, when the criterion of tool failure was volume of wear scar, also follow a straight line. Calculating for n and C we got the equation,

$$VT^{0.756} = 834$$

It would be very useful to compare the pin life equation found using volume of wear as the failure criterion with the tool life equation of the volume of flank wear as failure criterion. However it seems that metal cutting engineers are contented with the flank wear criterion itself. Inspite of careful search by the author, it was not possible to find readily any work where the constants n and C are evaluated on the volume criterion.

### 3.3.2 Effect of Feed

Effect of feed on "pin life" can be analysed by comparing Fig. 3.7 and Fig. 3.8. Fig. 3.8 shows the relation between "pin life" and rubbing speed at a feed rate of 0.1 mm/re.

The values obtained from the graph suggests the equation

$$VT^{.849} = 818$$

Whereas, for 0.05 mm/rev. feed rate, the equation found was

$$VT^{.854} = 1106$$

In both the above two cases pin diameter was 6.35 mm and other variables remained same, except the feed rate. This helped to analyse the effect of feed rate on "pin life". Comparison of the above two equations reveals that effect of feed rate on n is negligible but has considerable effect on C. This nature is similar to the cutting tool wear. "pin life" was found to be more for lower feed rate than in higher feed rate similar observation as available in cutting. The above analysis suggests that "pin life" also follows the equation of the form

$$VT^{n_f m} = C$$

where, f is the feed rate and n, m, C are empirical constants. The exact value of these constants for simple rubbing mechanism can be obtained by more experiments with different feed rates keeping all other variables constants.

### 3.3.3 Effect of Pin Radius

The effect of pin radius on "pin life" can be analysed from Fig. 3.7 and Fig. 3.9. The rubbing times corresponding to 5 mm wear scar length have been taken from Fig. 3.4 and plotted

in Fig. 3.9 with the corresponding velocities. The variation of "pin life" with rubbing velocity follows a straight line as in the previous cases. In both the two cases (Fig. 3.7 and Fig. 3.9) feed rate was 0.05 mm/rev. but having two different diameter pins as 6.35 mm and 4.4 mm, the other variables remained same. Calculation of  $n$  and  $C$  from Fig. 3.9 and Fig. 3 suggest the equations

$$VT^{0.643} = 338 \quad (\text{for pin dia.} = 4.4 \text{ mm})$$

$$VT^{0.854} = 1106 \quad (\text{for pin dia.} = 6.35 \text{ mm})$$

These relations show that the diameter of the pin has considerable effect on "pin life". Bigger diameter pin has got more life than the smaller diameter pin. The  $V_{60}$  values for 6.35 mm and 4.4 mm diameter pins are calculated to be 33.51 m/min. and 24.29 m/min. respectively. This has been plotted in Fig. 3.11. The trend matches with the trend in cutting provided pin diameter is replaced by cutting tool nose radius. In cutting it has been observed [28, 29] that with increase in nose radius of the tool, tool life increases or on the other hand decrease in nose radius decreases the  $V_{60}$  value. Comparison between the above two equations reveals that in crossed-cylinder rubbing, "pin life" follows an equation of the form,

$$VT^n = CR^m$$

where R is the pin radius and n, m, C are empirical constants. The nature of the equation is same as found in cutting where R has been replaced by nose radius.

In Chapter 2 it has been discussed with the help of Eq. 2.7 and Eq. 2.8 that decrease of nose radius causes decrease of Taylor's constant C. By comparing the two pin life equations with different diameters, it is seen that smaller diameter pin causes smaller value of the constant C as in cutting process. Therefore it can be concluded that effect of nose radius on tool life can be simulated by the effect of pin diameter provided proper selection of the diameter is made.

### 3.3.4 Taper Rubbing Test

It has been discussed in Chapter 1 that if the cutting tool life follows  $VT^n = C$  type of equation within a particular range of cutting speed then the constants n and C can also be found out by rapid taper turning test. As in the present work it has been found that the "pin life" also follows the same type of equation, it has been attempted to find out n and C by taper rubbing test.

For this purpose a 50 cm long taper was made having the semi-taper angle of  $3^\circ$ . Two tests have been performed at 250 and 400 r.p.m. at a fixed feed rate of 0.05 mm/rev. and over the same taper length.

Using Eq. 1.2 and Eq. 1.3, the constants n and C are calculated as 0.872 and 928 respectively. Thus the pin life equation can be written as

$$VT^{0.872} = 928$$

It is obviously clear that the test yields the values of n and C close to the values obtained in conventional rubbing test. This is a comfortable situation and suggests that the taper rubbing test can actually be a substitute for taper turning test provided it yields the values of n and C in the range obtained in actual cutting tests.\*

### 3.3.5 Coefficient of Friction

Variation of the coefficient of friction with rubbing velocity are plotted in Fig. 3.12. The value of the coefficient of friction decreases with increase in rubbing velocity. This can be explained by the following Bowden and Tabor model.

$$\text{Frictional resistance } F = \tau A_r + P$$

where,  $\tau$  = Shear stress required to rupture weld.

$A_r$  = Real area of contact.

P = Plowing component of friction force.

$$\text{So, the friction coefficient } \mu = \frac{F}{N} = \frac{\tau}{H} + \frac{P}{N}$$

where, Normal load,  $N = A_r \times H$

\* The values of n for H.S.S. and M.S. combination lie within 0.1 to 0.2 and value of C is around 200 m/min.

At very high sliding speeds, temperature generation is more which results decrease of the shear strength of the metal. As a result friction coefficient decreases with increase in sliding speed. Although hardness H also decreases with temperature rise but the decrease of  $\tau$  is more in comparison to H which results a net decrease of the friction coefficient. So the overall effect of increasing rubbing velocity causes coefficient of friction to decrease.

### 3.3.6 Calculation of Activation Energy for Resulting Wear

Any rate process can be expressed by means of Arrhenius equation which is of the form

$$\text{rate} = \text{constant} \times e^{-U/RT}$$

in which U is the activation energy in calories per mole, R is the gas constant (1.98 Cal/mole  $^{\circ}\text{K}$ ) and  $\theta$  is the absolute temperature in  $^{\circ}\text{K}$ .

It is well established that wear rate can also be expressed in a similar manner as

$$W = \frac{Z_0 N V_s}{H} \exp\left(\frac{-U}{RT}\right)$$

where, W = volume of wear/min.

N = normal load

$V_s$  = relative velocity.

$H$  = Hardness at room temperature  
 $\theta$  = Operating temperature  
 $U$  = Activation energy of the process  
 $R$  = Universal gas constant  
 $Z_0$  = Wear constant.

The equation can be rewritten as,

$$\ln \frac{W}{V_s} = \ln \left( \frac{Z_0 N}{H} \right) - \frac{U}{R} \cdot \frac{1}{\theta}$$

If in a wear experiment, the values of  $\ln \frac{W}{V_s}$  are plotted against  $\frac{1}{\theta}$  then the result should yield a straight line if the wear process is predominantly of adhesion type. In that case the slope of the straight line  $\frac{U}{R}$  is a measure of activation energy.

The results of the present work are plotted in Fig. 3.13. Here the temperature at the interface of the sliding pair have been calculated by the Bowden and Thomas [34] equation, given as

$$\theta = \frac{.236 NV_s \mu}{l [k_A + 0.88 k_B \left( \frac{V_s}{k_B} \right)^{0.5}]}$$

where,  $\mu$  = coefficient of friction

$l$  = length of the slider

$k_A, k_B$  = thermal conductivities of slider (A) and body (B) respectively,

$\bar{k}_B$  = thermal diffusivity of body (B).

It can be seen from Fig. 3.13 that the results of the plotting yields a straight line. This suggests that the wear mechanism was predominantly of adhesion type. Calculation for the slope yields,  $\frac{U}{R} = 16000\text{K}$  which results  $U = 31.68 \text{ K.Cal/mole}$ . It has been found that activation energy for self diffusion is a function of strain rate.

Hiranto et al. [32] have shown that at very small strain rate ( $10^{-6}/\text{sec}$ ), the activation energy for self diffusion  $U$  in compression tests is about  $50 \text{ K.Cal/mole}$  for alpha iron whereas at the strain rate of  $10^{-2}/\text{sec}$  they obtained  $U$  to be only  $19.2 \text{ K.Cal/mole}$ . Values of activation energy proposed by several metal cutting researchers fall in the range of  $30-50 \text{ K.Cal/mole}$ . The calculated value in the present work falls within the same range. This is another indication that the mechanism of rubbing wear is similar to cutting tool flank wear.

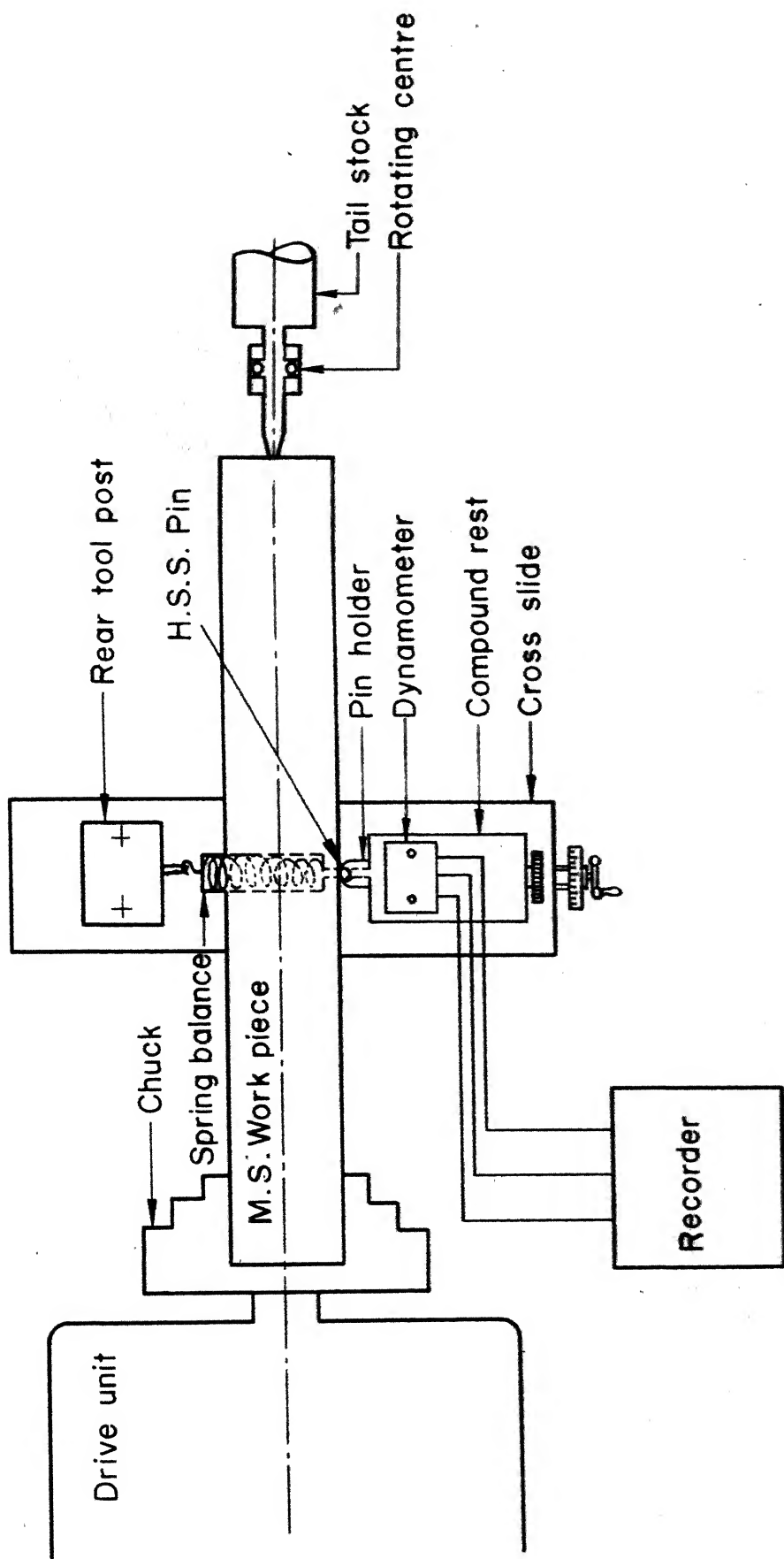


**Fig. 3.1** Schematic view of the experimental set-up

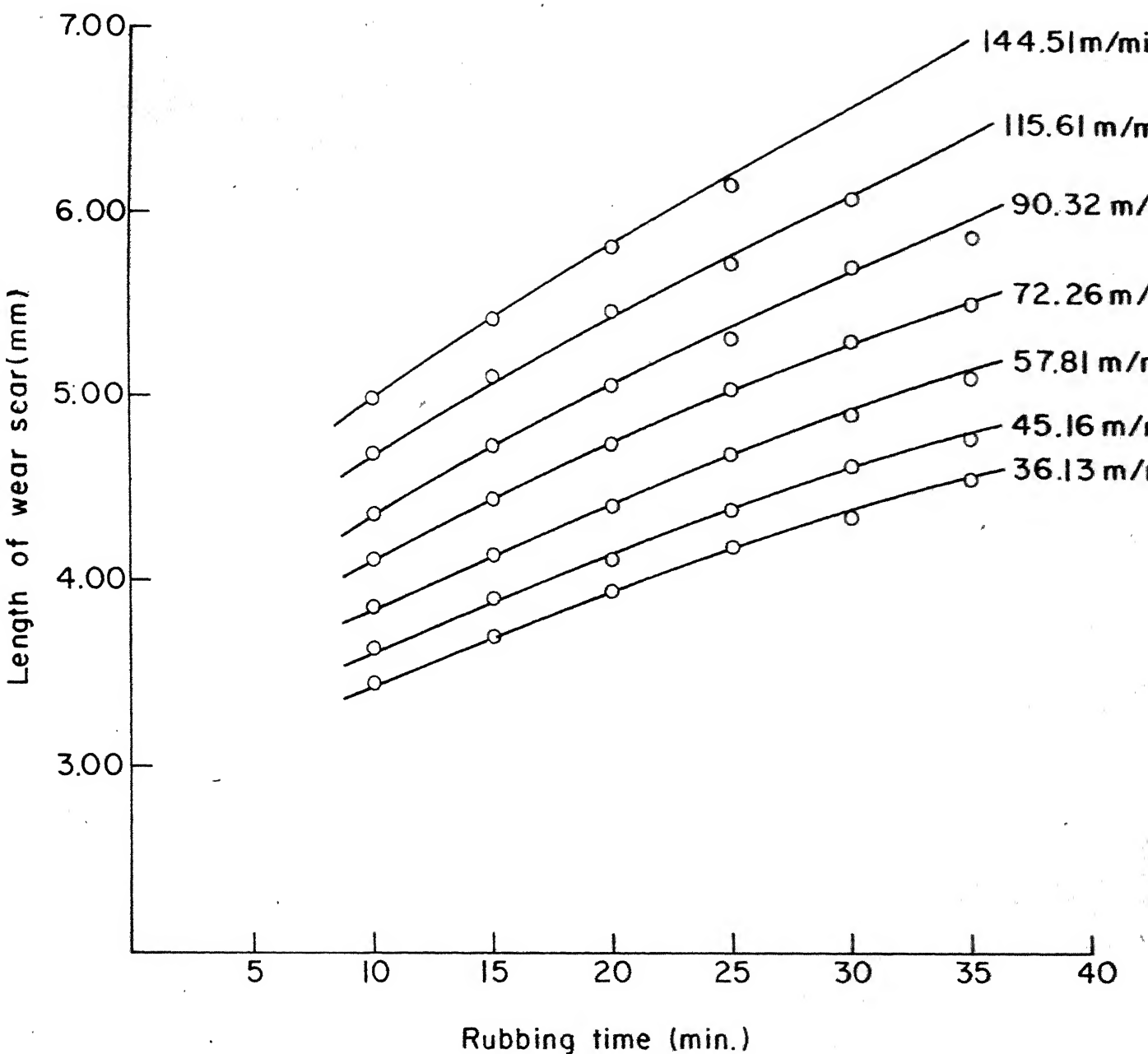


Fig.3.2

Variation of wear scar length with rubbing time at different rubbing velocities.

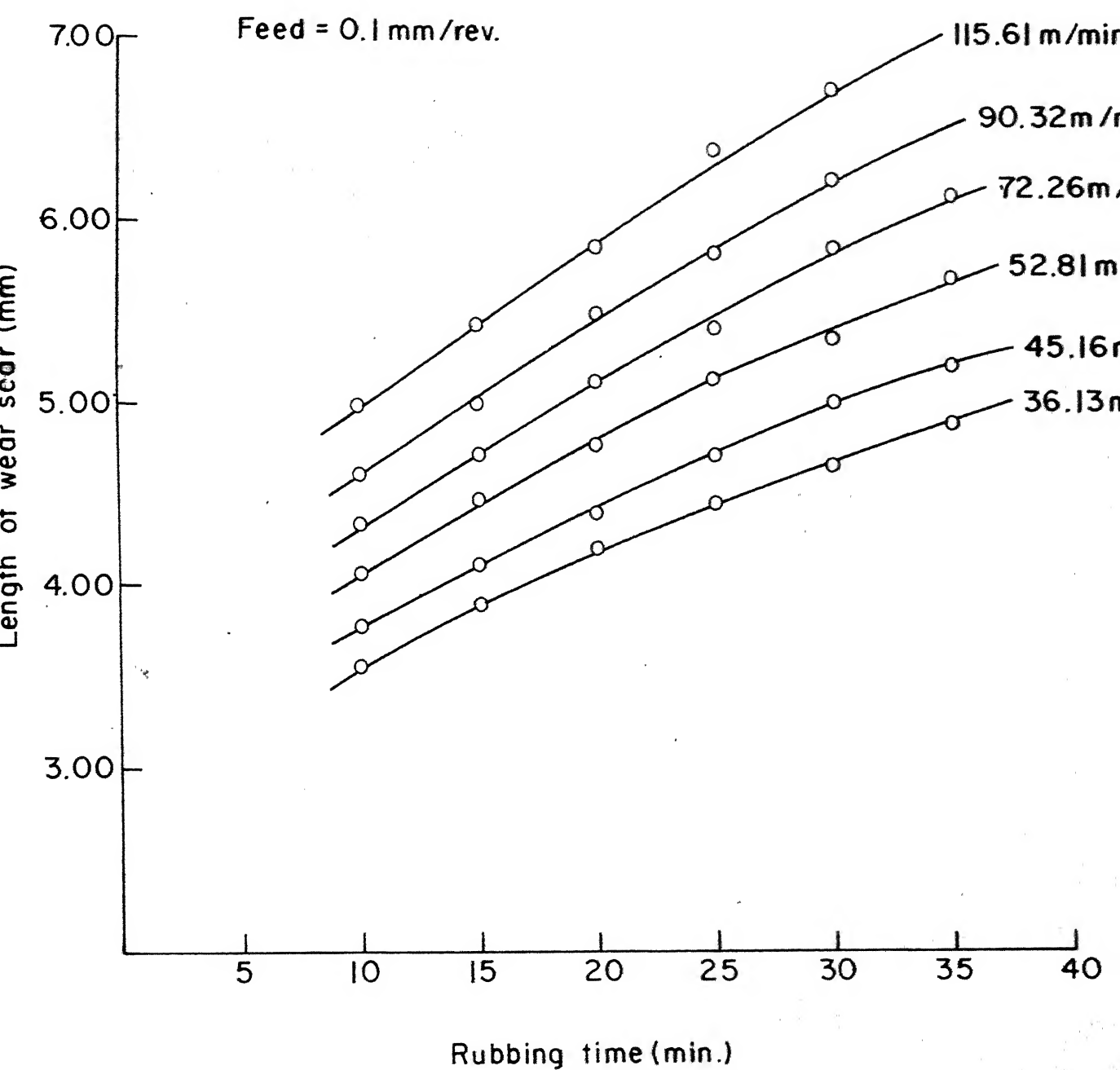


Fig. 3.3 Variation of wear scar length with rubbing time at different rubbing velocities.

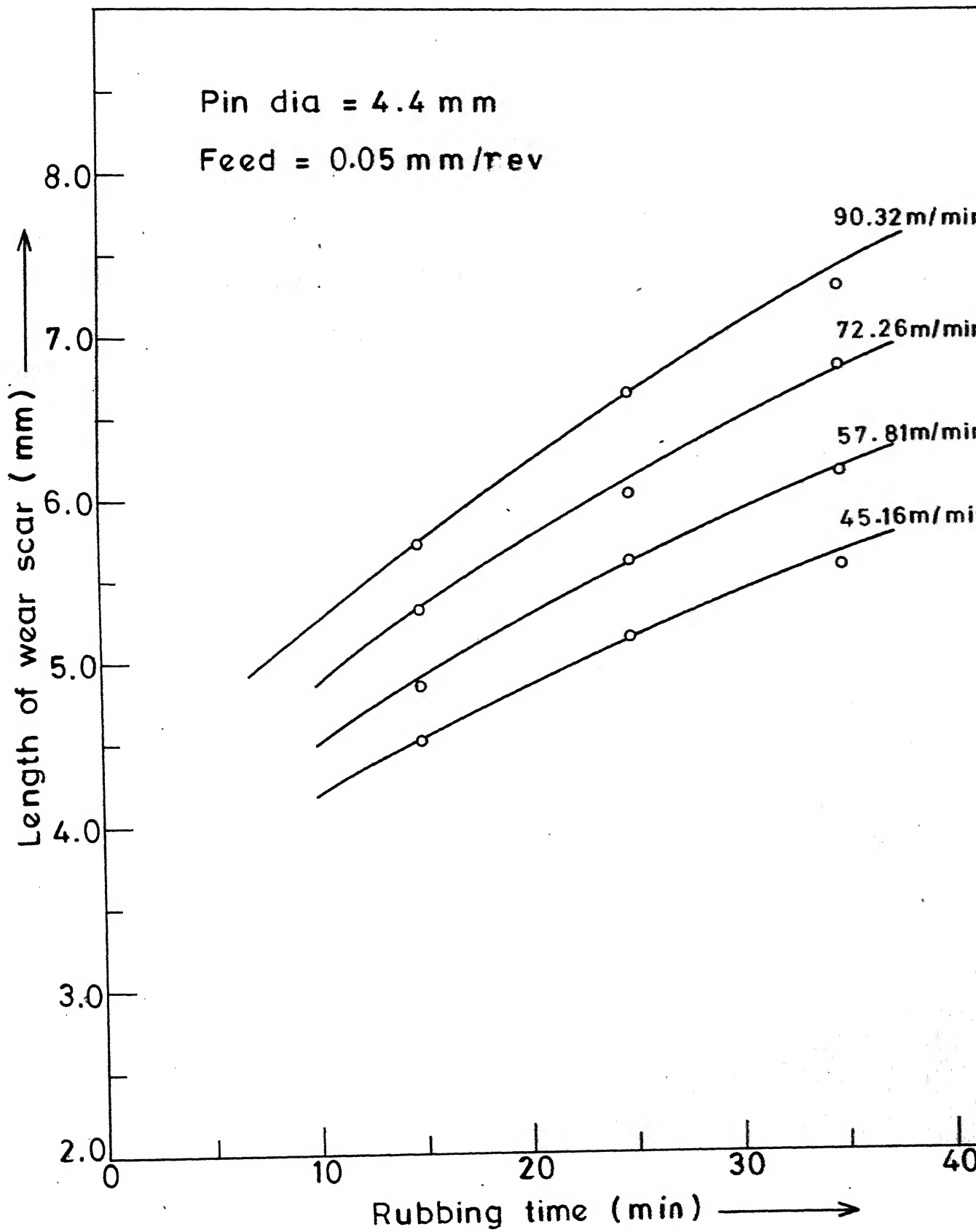


Fig. 3.4 Variation of wear scar length with rubbing time at different rubbing velocities.

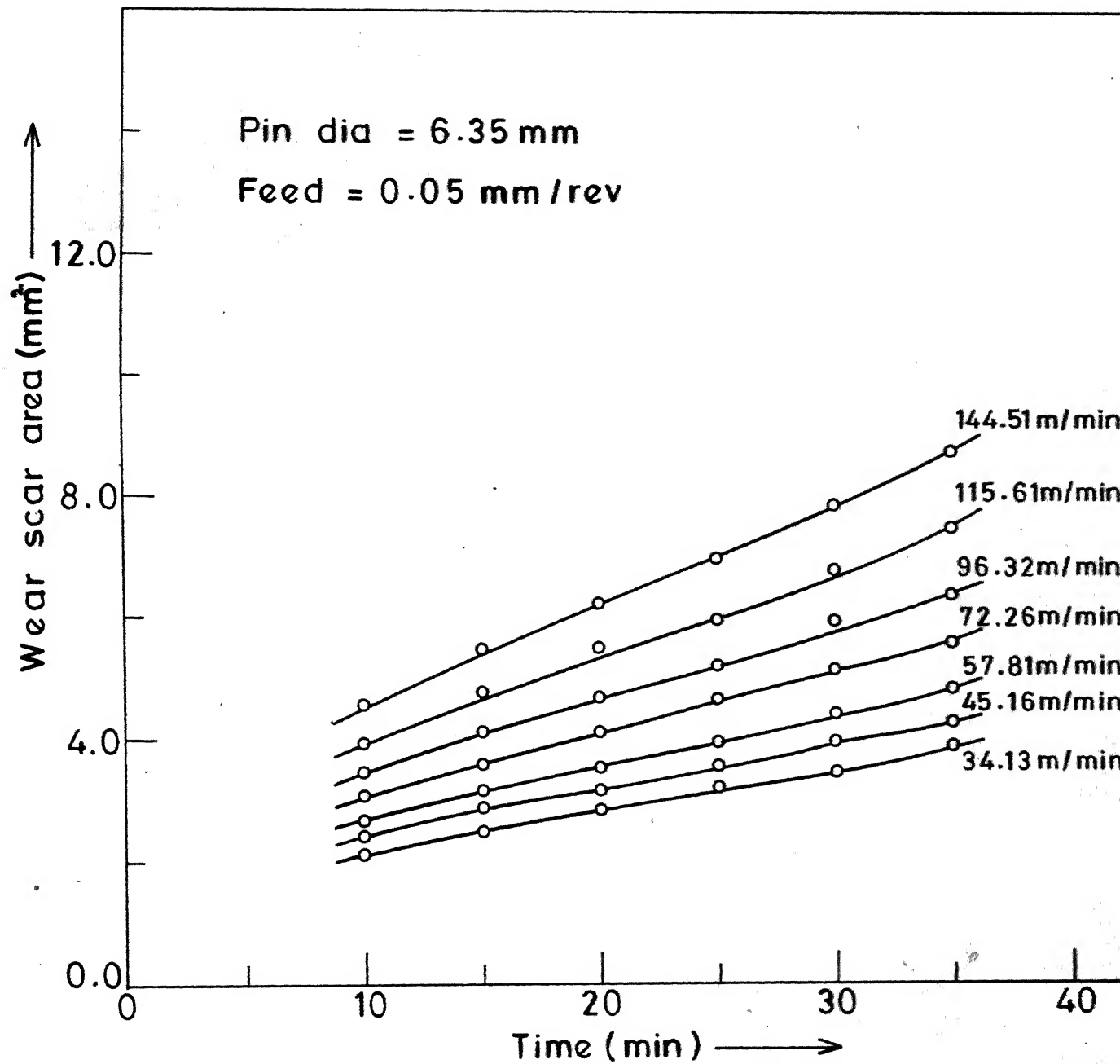


Fig. 3.5 Variation of wear scar area with time with different rubbing velocities.

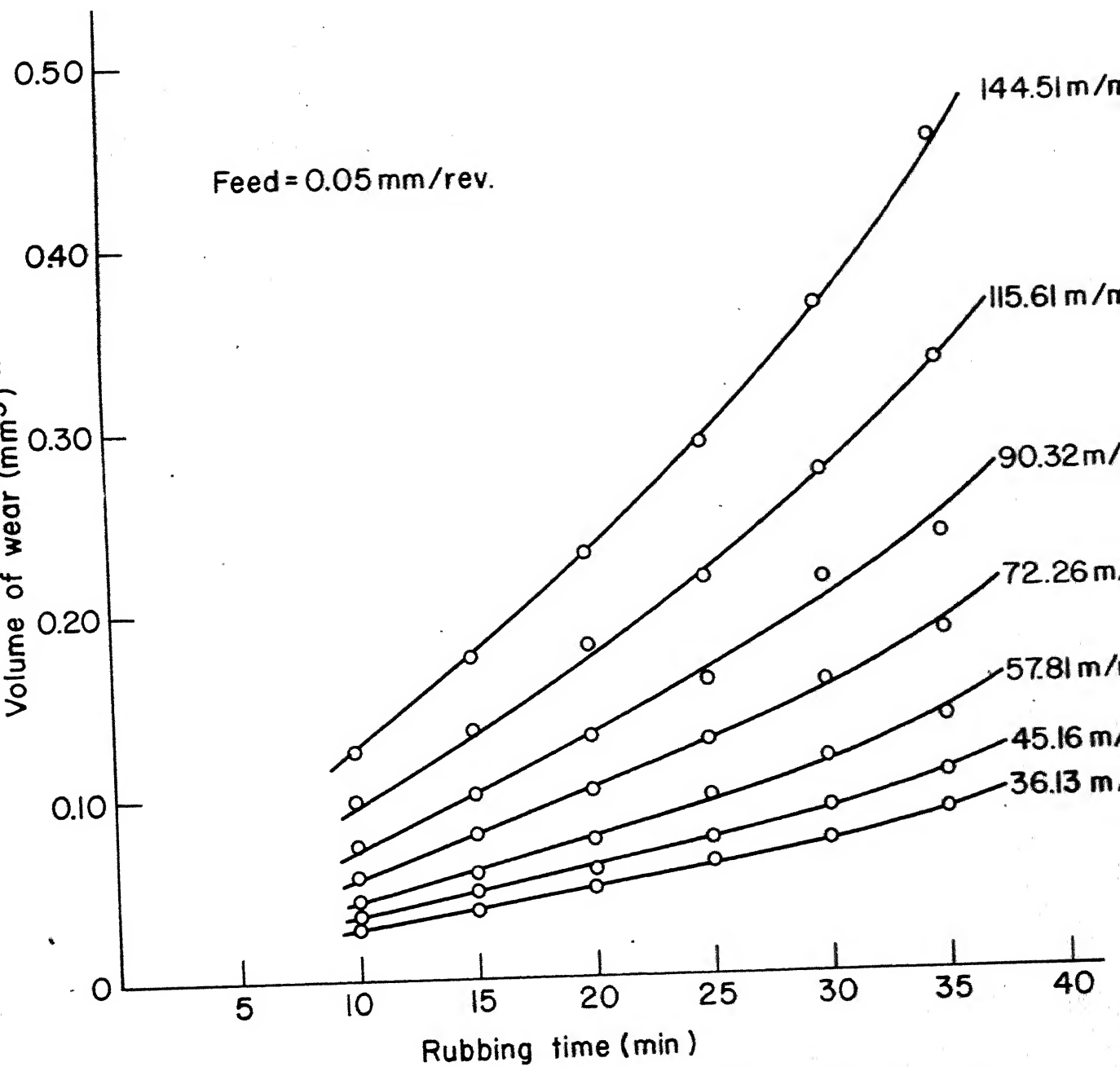
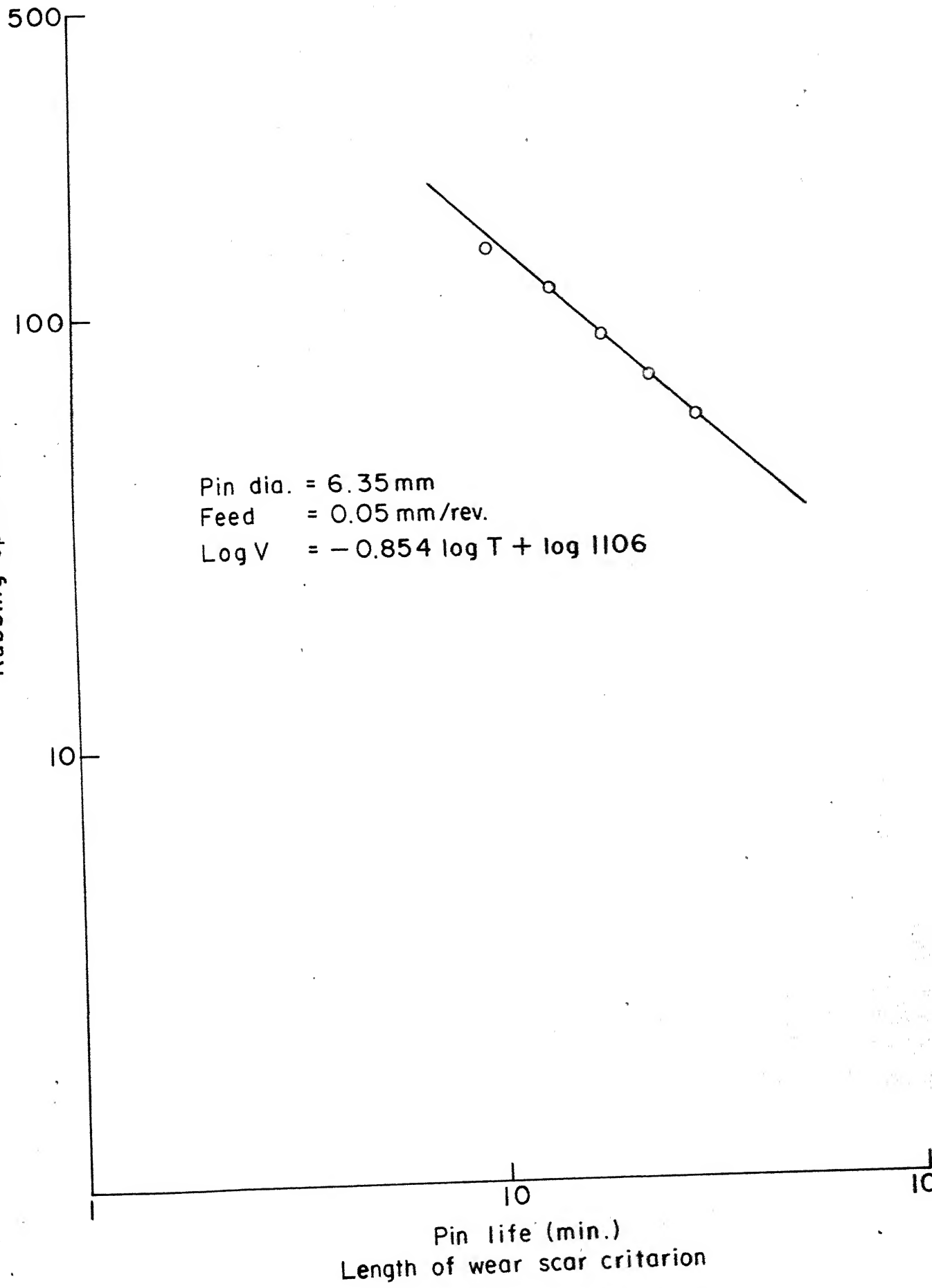


Fig. 3.6 Variation of volume of wear with rubbing time at different rubbing velocities

Rubbing speed (m/min.)



Rubbing speed (m/min.)

500

100

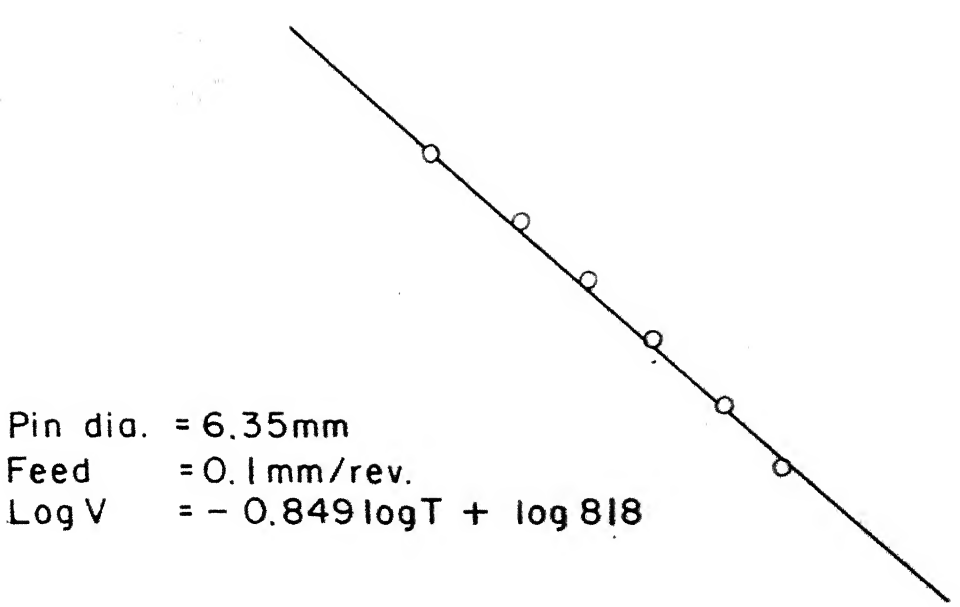
10

10

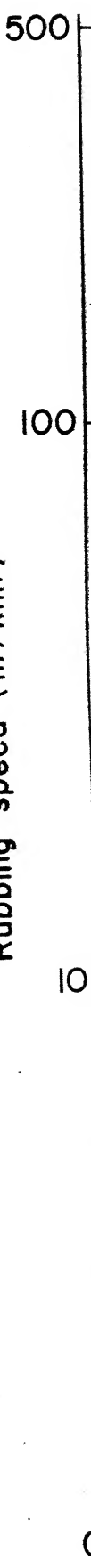
Pin life (min.)

Pin dia. = 6.35mm  
Feed = 0.1 mm/rev.  
 $\log V = -0.849 \log T + \log 818$

Length of wear scar criterion



Rubbing speed (m/min)

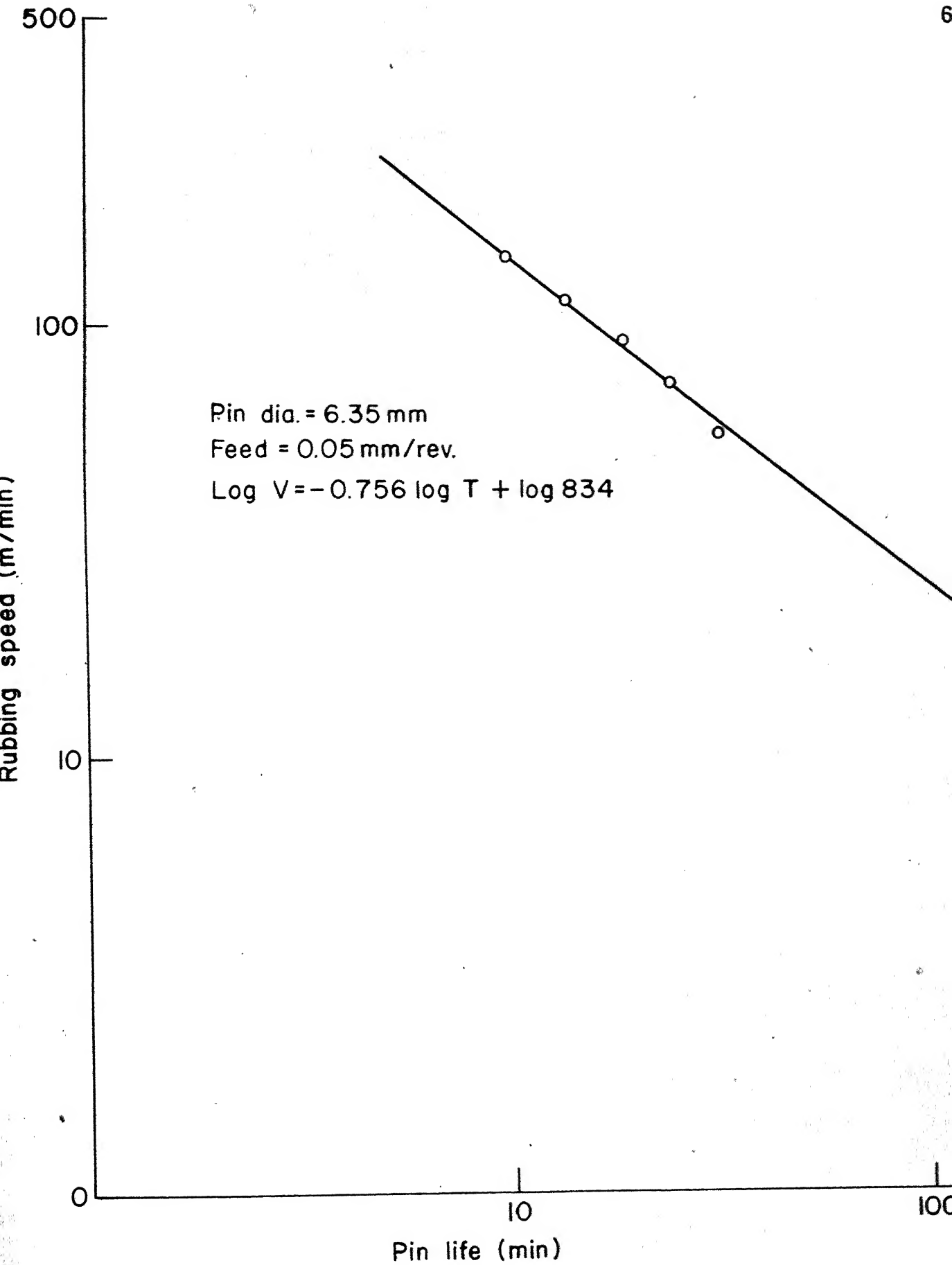


Pin dia. = 4.4 mm

Feed = 0.05 mm/rev.

$$\log V = -0.643 \log T + \log 338$$

Length of wear scar criterion



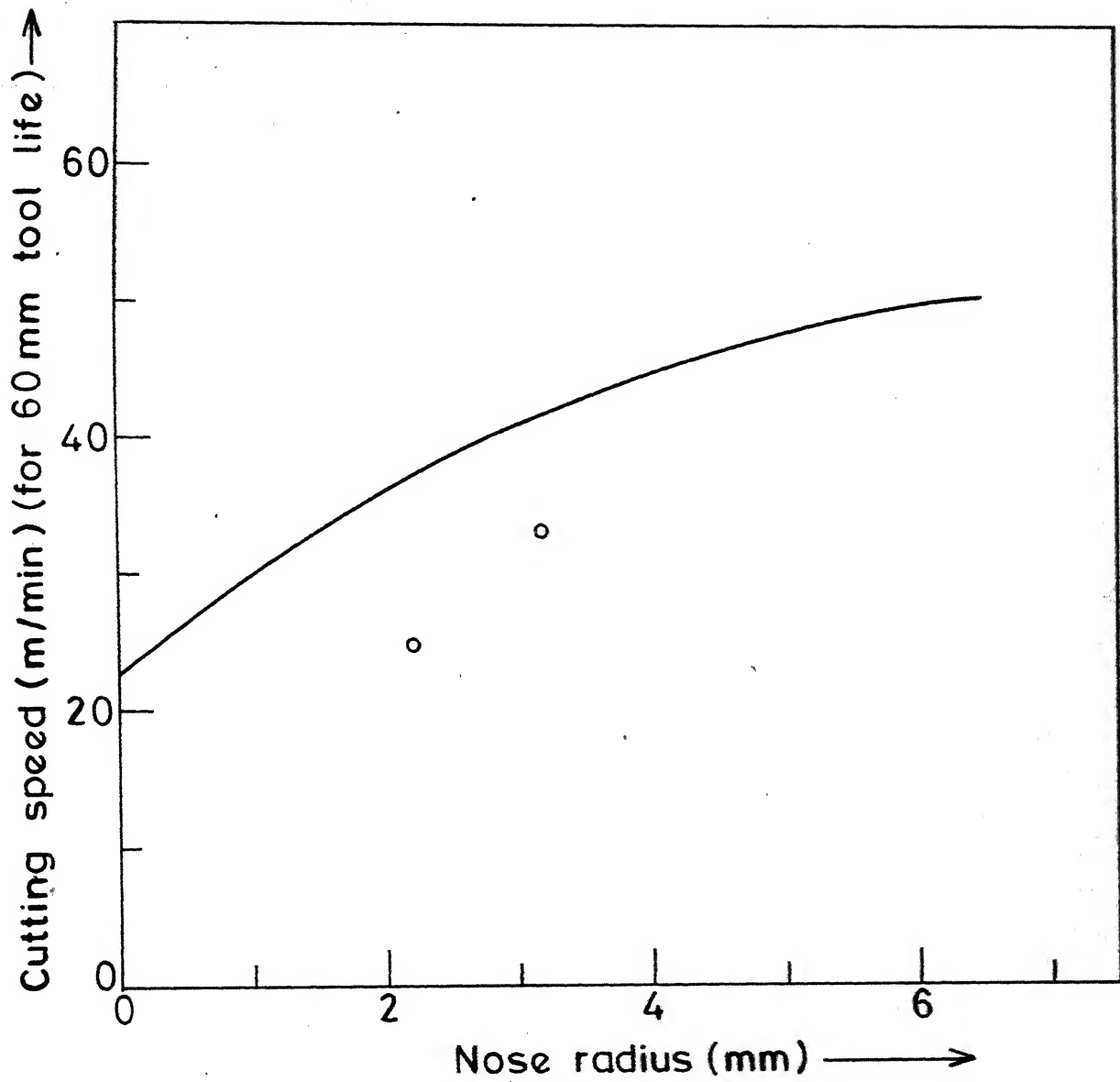


Fig. 3.11 Variation of tool life with nose radius.

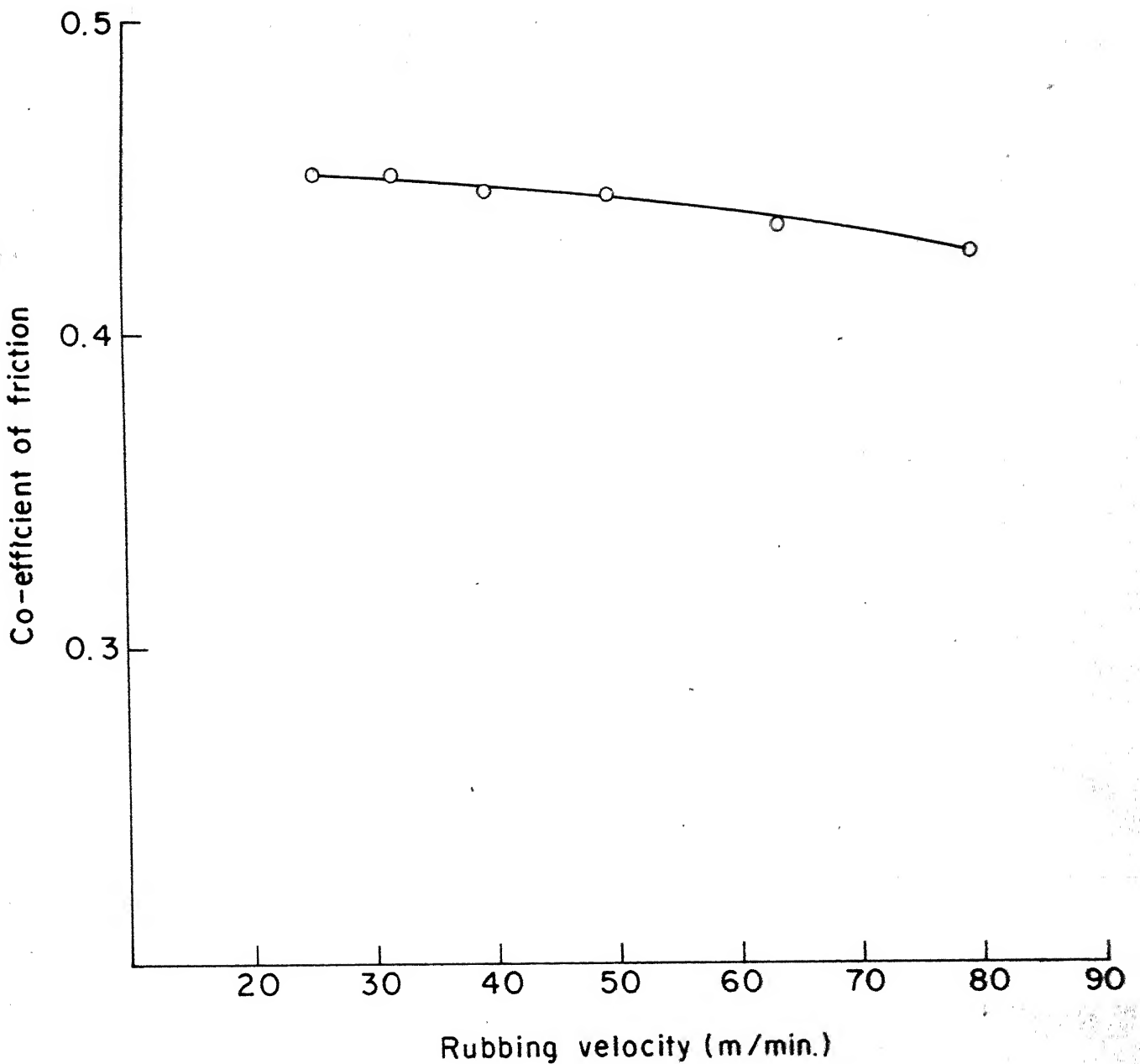


Fig.3.12 Variation of co-efficient of friction with rubbing velocity.

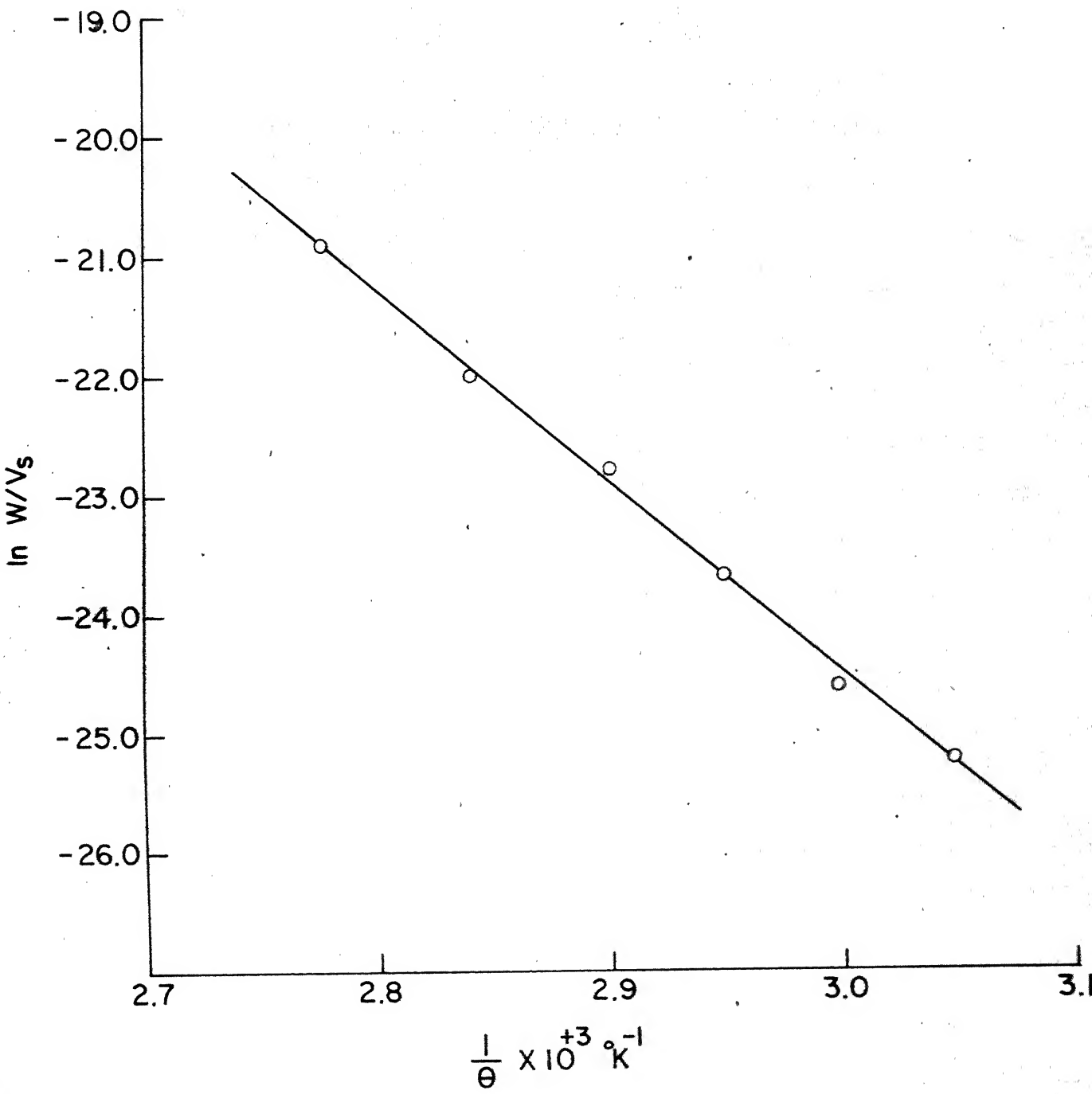


Fig.3.13 Variation of wear rate per unit distance with  $\frac{1}{\theta}$

CHAPTER IV  
CONCLUSIONS AND SUGGESTIONS FOR FUTURE WORK

On the basis of the experimental results and discussions presented previously, the following conclusions can be drawn.

- (i) Qualitatively there is a great similarity between the flank wear behaviour and the wear pattern obtained in the crossed-cylinder system.
- (ii) A "pin-life" equation similar to Taylor's tool life equation is obtainable in the crossed cylinder system.
- (iii) "pin-life" constants ( $n$  and  $C$ ) are larger than their counterparts in the Taylor's tool life equation and nose radius.
- (iv) Effect of feed and nose radius on "pin life" is similar to that observed in tool-life studies.
- (v) Effect of side cutting edge angle on tool life (which is influenced by nose radius) in cutting is also observable in pin life through change in pin diameter.

Some more work in the same line have been suggested to justify whether the present work can finally be adopted as a standard method for tool life testing.

A hot taper rubbing test conducted under adjustable conditions of interface temperature and normal load (which determine the depth of indentation) would be a quick method of arriving at values of  $n$  and  $C$  close to those existing in cutting.

This would then expectedly, lead to a standard set of values of heating current, pin radii and normal load for performing rubbing test for obtaining n and C values. Further work is essential in the direction to bring this part of the work to a reasonable conclusion. Due to the nature of the task involved, it could not form part of the present work and is strongly recommended as a future work.

## REFERENCES

1. N.H. Cook, "Manufacturing Analysis", Addison-Wesley Publishing Co., Reading, Mass, 1966.
2. I. Finnie and M.C. Shaw, "The Friction Process in Metal Cutting", T.A.S.M.E., Vol. 78, 1956, pp. 1649-1657.
3. N.N. Zorev, "Metal Cutting Mechanics", Pergamon Press, Oxford, 1966.
4. F.P. Bowden and D. Tabor, "The Friction And Lubrication of Solids". Oxford University Press, 1950.
5. S. Kabayashi and E.G. Thomsen, "The Role of Friction in Metal Cutting", T.A.S.M.E., Series B, J. of Engg. for Ind., Vol. 82, Nov. 1960, pp. 324-332.
6. H. Takeyama and E. Usui, "The Effect of Tool-Chip Contact Area in Metal Machining", Trans. ASME, Series B, J. of Engg. for Ind., Vol. 81, 1959, pp. 139-151.
7. M.C. Shaw et.al., "Leaded Steel and the Real Area of Contact in Metal-Cutting", Trans. ASME, Vol. 79, 1957, pp. 1143-1154.
8. B.T. Chao and K.J. Trigger, "Cutting Temperature and Metal Cutting Phenomena", Trans. ASME, Vol. 73, 1951, pp. 777-793.
9. M. Kronenberg, "Metal Cutting Friction Coefficient Needs Reinterpretation", Tool Engineer, Vol. 32, 1953, p.49.
10. A.D. Sarkar, " Wear of Metals", Pergamon Press, Oxford, 1976.
11. M.C. Shaw and P.A. Smith, " Tool Wear Results from Several Causes", American Machinist, New York, Vol. 95, 1951, p. 100.
12. F.W. Taylor, " On the Art of Cutting Metals", Trans. ASME, Vol. 28, 1907, p. 31.
13. Kunio Uhera, "Characteristics of Tool Wear based on Volume of Flank and Crater Wear - A Proposal on the Measurement of Tool Life", Annals CIRP, Vol. 24, 1975, p. 59.
14. M. Kronenberg, " Machining Science and Application", Pergamon Press, Oxford.

15. Edmond E. Bisson, "Friction, Wear and Surface Damage of Metals as Applied by Solid Surface Films", Handbook of Mechanical Wear, Edited by C. Lipson and L.V. Colwell, The University of Michigan Press, pp. 35-55.
16. Toshio Sata, "Transience of the State of Wear by Repeated Rubbing", WEAR, Vol. 3, 1960, pp. 104-113.
17. J. Halling, "A Crossed-Cylinder Wear Machine and its Use in the Study of Severe Wear of Brass on Mild Steel", WEAR, Vol. 4, 1961, pp. 22-31.
18. B.N. Colding, "A Three Dimensional Tool Life Equation Machining Economics", Trans. ASME, Series B, J. of Engg. for Ind., Vol. 81, 1959, p. 239.
19. N.N. Zorev and N.I. Tashlitsky, "Effect of the Secondary Shear Zone on High-Speed Cutting Tools", Machinability (Proc. of a Conf. on Machinability), 1967, p. 31.
20. G. Barrow, "Tool Life Equation and Machining Economics", Proc. of 12th Int. MTDR Conf., Sept. 1971, pp. 481-493.
21. C.E. Kraus and R.R. Weddell, "Determining the Tool Life Cutting-Speed Relationship by Facing Cuts", Trans. ASME, Vol. 59, 1937, pp. 555-558.
22. V. Solaja, "Tool Life Testing by Facing in a Lathe", WEAR, Vol. 1, 1957, p. 512.
23. W.B. Heginbotham and P.C. Pandey, "Taper Turning Tests Produce Reliable Tool-Wear Equations", Proc. of Int. MTDR Conf., 1966, p. 515.
24. W.B. Heginbotham and P.C. Pandey, "A Variable Rate Machining Test for Tool Life Evaluation", Proc. of Int. MTDR Conf., 1967, p. 163.
25. T.S. Kiang and G. Barrow, "Determination of Tool Life Equation by Step Turning Test", Proc. of 12th Int. MTDR Conf., Sept. 1971, p. 379.
26. N.H. Cook, "Tool Wear and Tool Life", Trans. ASME, Series B, J. of Engg. for Ind., Vol. 95, 1973, p. 931.
27. D.R. Olberts, "A Study of the Effect of Tool Flank Wear on Tool Chip Interface Temperature", Trans. ASME, Series B, J. of Engg. for Ind., Vol. 81, 1959, p. 152.
28. G.C. Sen and A. Bhattacharyya, "Principles of Metal Cutting", New Central Book Agency, Calcutta, 1969.

29. Lawrence E. Doyle, "Manufacturing Processes and Materials for Engineers", PHI, New Delhi, 1975.
30. O.W. Boston, "A Bibliography of Metal Cutting", Part I, ASME, 1930, Part II, 1935.
31. M.K. Muju, "Effect of Magnetic Field on Wear", Ph.D. Thesis, I.I.T. Kanpur, 1975.
32. K. Hiranto, M. Cohen et al., "Self-Diffusion in Alpha Iron During Compressive Plastic Flow", Trans. Metall. Soc. AIME, 227 (1963) 950.
33. I.V. Rao, "Tool Wear and Tool Life at High Cutting Speeds", M.Tech. Thesis, I.I.T. Kanpur, Oct. 1976.
34. F.P. Bowden and P.H. Thomas, "The Surface Temperature of Sliding Solids", Proc. Roy. Soc., London, A223 (1954), p. 29.
35. E.G. Loewen et al., "Electric Strain Gauge Tool Dynamometers", Proc. SESA, Vol. VIII, No. 2, 1951, p. 1.
36. E.G. Loewen and N.H. Cook, "Metal Cutting Measurement and Their Interpretation", Paper presented at the Spring meeting of SESA, Ohio, April, 1954.
37. N.H. Cook et al., "Machine-Tool Dynamometers .... a current appraisal", American Machinist, May 10, 1954.

## APPENDIX

### 1. Dynamometer Design

The two basic factors which conflict each other for designing the force measurement dynamometer are sensitivity and rigidity. In order to make a dynamometer sensitive, it loses rigidity while to make a dynamometer rigid will cause loss of sensitivity. Moreover a dynamometer should be sufficiently stiff so as not to interfere with the cutting operation by causing excessive vibration and chatter. Loewen et al. [35] have discussed in details regarding the type of dynamometer that can be used in different machining processes. Loewen and Cook [36] have analysed the adoptability of using round and octagonal ring dynamometers for measuring the forces in metal machining. They found that the following equations are satisfactory for octagonal rings to estimate the strains at different face of it.

$$\epsilon_{(\text{centre})} = 0.7 \frac{V R}{E b t^2} \quad (4.1)$$

$$\epsilon_{(45^\circ \text{ face})} = 1.4 \frac{H R}{E b t^2} \quad (4.2)$$

where, V and H are the vertical and horizontal force components and b is the width and t is the thickness of the ring, E being the modulus of elasticity.

The vertical and horizontal deflection can be calculated as,

$$\delta_V = \frac{V R^3}{E b t^3} \quad (4.3)$$

$$\delta_H = 3.7 \frac{H R^3}{E b t^3} \quad (4.4)$$

where,  $\delta_V$  is the vertical deflection due to V and  $\delta_H$  is the horizontal deflection due to H. Cook et al. [37] have proposed an extended octagonal ring dynamometer for turning process. However in the present work, double octagonal ring dynamometer was designed to be used. Fig. A-1 shows the basic design of dynamometer. The maximum load capacity of loading (80 Kg radial) was calculated with Eq. 4.1 and Eq. 4.2. Semiconductor strain gauges were used to make it more sensitive. The calibration curve has been shown in Fig. A-2. Linearity was found in all the cases and there was no interacting signals among the forces.

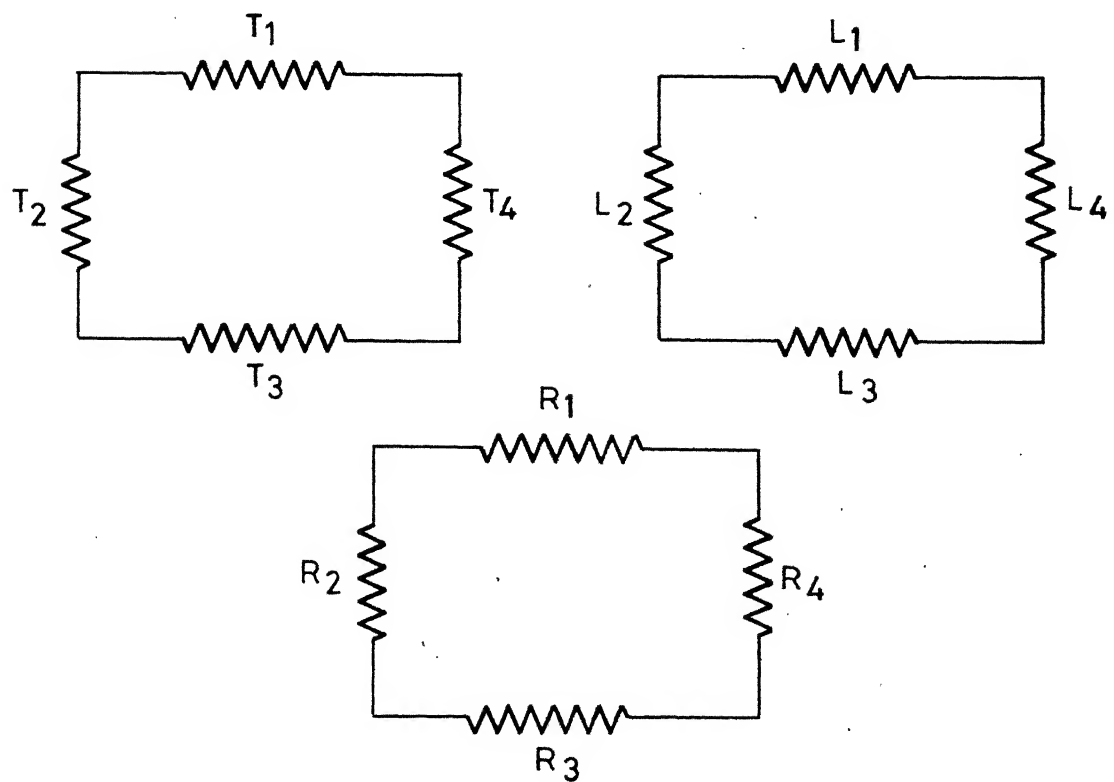
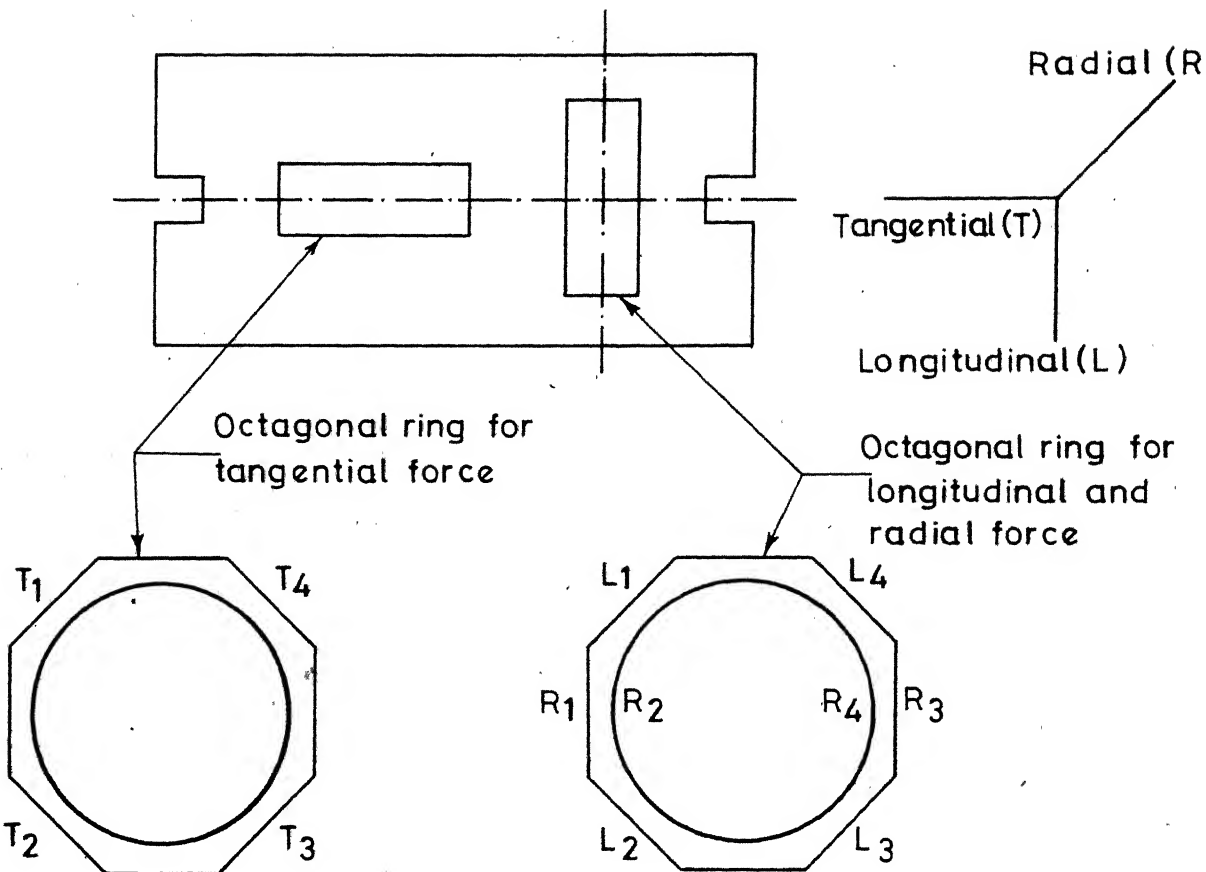


Fig. A-1 Dynamometer details.

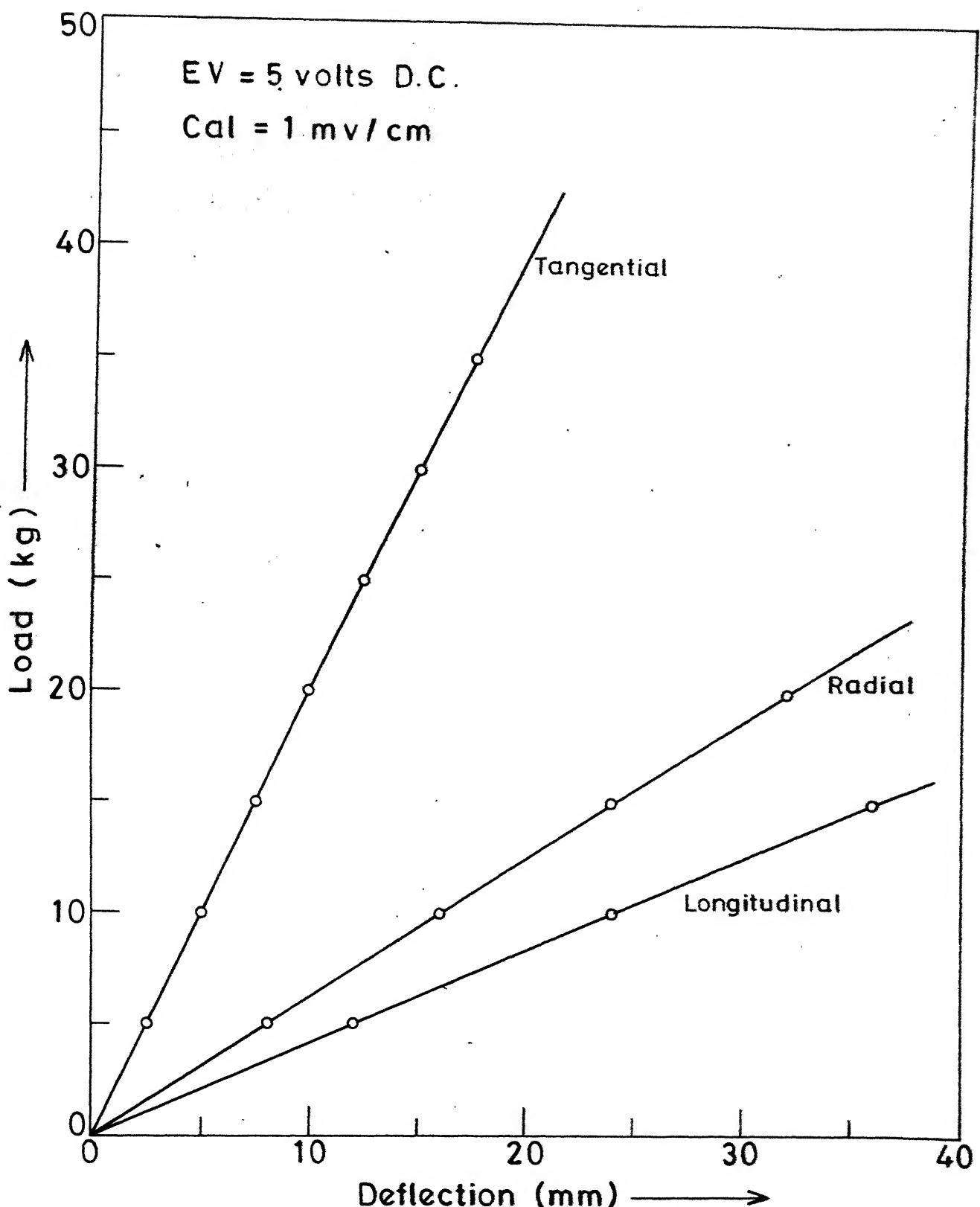


Fig. A-2 Calibration chart of dynamometer at a sensitivity of 0.02

## 2. Computer Programming

A computer program for calculating Eq. 3.3 and Eq. 3.4 is given below. The input data is length of the major axis of the wear scar. The output data are the surface area and volume of wear scar.

```

C      COMPUTING THE SURFACE AND VOLUME
C
DATA BR, SR, A/57.500, 3.175,0./
K=0
READ *, N,J
C J AND N ARE THE NO OF DATAS OF HT AND DIVISION BY TWO
PRINT 20
20 FORMAT(10X,'X',10X,'Y',10X,'HEIGHT',10X,'SURFACE',10X,'VOLU
19X, 3(1H-), 8X, 3(1H-),8X,8(1H-),8X, 9(1H-),8X(1H-))
1 READ *, PO
PO=PO/2.
HT=BR+SQRT(BR**2-PO**2)
K=K+1
B0=BR+SR-HT
B=SQRT(BR**2-(BR-HT)**2)
H=(B-A)/(2.*FLOAT(N))
P=SQRT(SR**2-(SR-HT)**2)
X=A
SUR=0.
VOL=0.
DO 25 I=1, N
X=X
Y=X+H
Z=X+2.*H
FX1=F(X,BR,SR,HT)
FX2=F(Y,BR,SR,HT)
FX3=F(Z,BR,SR,HT)
GX1=G(X,BR,SR,HT)
GX2=G(Y,BR,SR,HT)
GX3=G(Z,BR,SR,HT)
SUR=SUR + (H/3.) * (FX1+4.*FX2+FX3)
VOL=VOL + (H/3.) * (GX1+4.*GX2+GX3)
X=X+2.*H
25 CONTINUE
PRINT 30, P, B, HT, SUR, VOL

```

```
30 FORMAT(6X, F7.3, 4X, F7.3, 7X,F7.5,8X,F9.4,8X,F9.8/ )
IF(K.GE.J)GO TO 40
GO TO 1
STOP
END

C
C      FUNCTION SUBPROGRAM SURFACE
FUNCTION F(Y,BR,SR,HT)
RR=BR+SR-HT
RY=(RR-SQRT(BR**2-Y**2))
FY=SQRT(SR**2-RY**2)
F=4.*BR*FY/SQRT(BR**2-Y**2)
RETURN
END  ◎

C
C      FUNCTION SUBPROGRAM VOLUME
FUNCTION G(Y,BR,SR,HT)
RR=BR+SR-HT
RY=(RR-SQRT(BR**2-Y**2))
FY=SQRT(SR**2-RY**2)
G=4.*((FY*SQRT(BR**2-Y**2)-RR*FY+(SR**2/2.)*ASIN(FY/SR)+(F Y,
1*SQRT(SR**2-FY**2)))
RETURN
END  ◎
```